

# Low Mach number preconditioning techniques for Roe-type and HLLC-type methods for a two-phase compressible flow model

Marica Pelanti<sup>a,\*</sup>

<sup>a</sup>*Institute of Mechanical Sciences and Industrial Applications, UMR 9219 ENSTA ParisTech - EDF - CNRS - CEA, Université Paris-Saclay, 828, Boulevard des Maréchaux, 91762 Palaiseau Cedex, France*

---

## Abstract

We describe two-phase flows by a six-equation single-velocity two-phase compressible flow model with stiff mechanical relaxation. In particular, we are interested in the simulation of liquid-gas mixtures such as cavitating flows. For the numerical approximation of the homogeneous hyperbolic portion of the model equations we have previously developed two-dimensional wave propagation finite volume schemes that use Roe-type and HLLC-type Riemann solvers. These schemes are very suited to simulate the dynamics of transonic and supersonic flows. However, these methods suffer from the well known difficulties of loss of accuracy and efficiency encountered by classical upwind finite volume discretizations at low Mach number regimes. This issue is particularly critical for liquid-gas flows, where the Mach number may range from very low to very high values, due to the large and rapid variation of the acoustic impedance. In this work we focus on the problem of loss of accuracy of standard schemes related to the spatial discretization of the convective terms of the model equations. To address this difficulty, we consider the class of preconditioning strategies that correct at low Mach number the numerical dissipation tensor. First we extend the approach of the preconditioned Roe-Turkel scheme of Guillard–Viozat for the Euler equations [Computers & Fluids, 28, 1999] to our Roe-type method for the two-phase flow model, by defining a suitable Turkel-type preconditioning matrix. A similar low Mach number correction is then devised for the HLLC-type method, thanks to a novel reformulation of the HLLC solver. We present numerical results for two-dimensional liquid-gas channel flow tests that show the effectiveness of the proposed preconditioning techniques. In particular, we observe that the order of pressure fluctuations generated at low Mach number regimes by the preconditioned methods agrees with the theoretical results inferred for the continuous relaxed two-phase flow model by an asymptotic analysis.

*Keywords:* Two-phase compressible flows, liquid-gas mixtures, mechanical relaxation, finite volume schemes, Riemann solvers, low Mach number, Turkel’s preconditioning.

*2000 MSC:* 65M08, 76T10

---

## 1. Introduction

We describe two-phase flows by a six-equation single-velocity two-phase compressible flow model with stiff pressure relaxation [1, 2]. In particular, we are interested in the simulation

---

\*Corresponding author. Tel.: +33 1 69 31 98 19; Fax: +33 1 69 31 99 97.

Email address: marica.pelanti@ensta-paristech.fr (Marica Pelanti)

of liquid-gas mixtures such as cavitating flows, which are found in many systems of different areas of engineering, such as naval and aerospace technologies and the nuclear industry. In the modelling of these flows it is important to take into account the compressibility of all the phases, gas as well as liquid, to correctly describe acoustic perturbations and the wave dynamics. This has motivated our study of a two-phase flow model that treats each phase as a compressible fluid. This model, which we first considered in [3, 1], is a variant of the six-equation two-phase flow model with stiff pressure relaxation of Saurel–Petitpas–Berry [2], and it belongs to a class of compressible multiphase flow models stemming from the original work of Baer–Nunziato [4], see e.g. the models in [5, 6].

We numerically approximate the two-phase system by a fractional step algorithm, which alternates between the solution of the homogeneous hyperbolic portion of the equations through wave propagation Godunov-type finite volume schemes, and the solution of a system of ordinary differential equations that takes into account the stiff pressure relaxation source terms. For the solution of the homogeneous two-phase system we have proposed in [1] schemes that use Roe-type and HLLC-type Riemann solvers. These numerical methods prove to be very efficient to simulate wave propagation phenomena and shocks in transonic and supersonic flows. Unfortunately, these schemes suffer from the well known difficulties encountered by upwind finite volume discretizations for compressible flows at low Mach number: dramatic loss of accuracy, failure of convergence to the correct solution, very high computational cost when standard time-explicit schemes are used, since the CFL stability condition for these schemes demands a time step of the order of the Mach number. These issues are particularly critical for liquid-gas flows, since here the Mach number may range from very low values in the weakly compressible liquid medium to very large values in the gas and liquid-gas mixture zones. Due to the large and rapid variation of the acoustic impedance in these flows, it is important to be able to accurately describe a wide range of Mach number regimes.

There exists very abundant literature on the topic of low Mach number flows, including theoretical studies on the incompressible limit of the compressible flow equations, analyses of the failure of some classical compressible flow solvers, and formulations of numerical methods suited for low Mach number regimes by a variety of approaches [7, 8, 9, 10, 11, 12, 13, 14, 15, 16, 17, 18, 16, 19, 20, 21, 22, 23, 24, 25]. Note that most of the studies on this topic are devoted to the case of single-phase flows (Euler or Navier-Stokes equations), while theoretical and numerical work on multiphase flow models is still limited in the literature, cf. e.g. [26, 27, 28, 29, 30]. This paper will focus solely on the problem of loss of accuracy at low Mach number, which is related to the spatial discretization of the convective terms of the considered model equations. In particular the problem was examined in depth for Godunov-type schemes for the Euler equations by Guillard, Murrone and Viozat in a series of papers [12, 13, 31]. In [12] the authors explain via an asymptotic analysis that the loss of accuracy is linked to the generation in the discrete solutions of pressure fluctuations of the wrong order of magnitude in the Mach number, with respect to the behavior of the continuous flow model. In [12] the proof is rigorously given for the Roe’s scheme. A powerful remedy to cure the accuracy problem of upwind finite volume schemes is preconditioning of the numerical dissipation term. Preconditioning techniques were originally introduced [9, 32] to accelerate convergence to a steady state and first used for low-speed steady state computations [10, 33, 34]. Preconditioning consisted of a matrix multiplying the time derivative term with the effect of reducing the disparity of the eigenvalues corresponding to the convective and acoustic modes, thus removing the stiffness of the equations. These techniques were not suited for time-dependent problems. It was then observed that preconditioning improves not only convergence but also accuracy of the steady

state solution for low Mach number problems [34]. This evidence led to the development of preconditioning strategies that do not alter the time derivative term as in the first approaches but act only on the upwind dissipation term in order to cure the accuracy problem while retaining consistency in time [35, 12, 13], thus allowing the simulation of unsteady flows. In this paper we consider this class of preconditioned methods. Note that these methods remain very inefficient in time [36] when explicit time integrations are used, and suitable time discretizations must be employed. However here we will not address this issue, which is nonetheless an important point of our planned work. Most of the low Mach number strategies that alter the dissipation term to improve accuracy have been conceived for approximations of the single-phase Euler equations [35, 12, 13, 20]. Some methods have also been developed for simple homogeneous mixture models [37, 38, 39, 40], which describe a two-phase medium as a single fluid governed by a set of equations formally monophasic. Work on preconditioning techniques for genuine multiphase compressible flow models of Baer–Nunziato type like the model that we consider is still scarce in the literature. The work of Murrone and Guillard [28] was the first to study theoretically at the continuous level the low Mach number behavior of the five-equation single-velocity single-pressure two-phase flow model of Kapila *et al.* [5], and to introduce a preconditioned method for this two-phase system based on an acoustic Riemann solver. More recently some preconditioning strategies have been proposed for similar two-phase flow models [29, 30].

Following the work of Guillard, Viozat and Murrone [35, 12, 28], the aim of our work has been to devise preconditioning techniques for the Roe-type and HLLC-type schemes that we have previously developed for our two-phase flow model, and to provide further insight on the accuracy problem for the two-phase case by examining the low Mach number behavior of continuous and discrete solutions of the equations. The main result of our studies has been the extension of the Roe-Turkel scheme of Guillard–Viozat [12] for the Euler equations to our original Roe-type scheme for the two-phase flow model, via the definition of a suitable Turkel-type preconditioner acting on the numerical viscosity matrix. Then, thanks to a novel reformulation of the HLLC Riemann solver that reveals the mathematical analogy of its wave structure with the one of the Roe solver, we were able to extrapolate the approach of the Roe-Turkel method of [12] to HLLC-type discretizations and obtain an HLLC-Turkel method for the two-phase flow model. A detailed study of this new HLLC-Turkel technique for the classical single-phase Euler equations will be presented in a separate work. Two-dimensional computations of low Mach number channel flow problems show the effectiveness of the proposed preconditioning techniques. In particular, we observe that the order of pressure fluctuations generated at low Mach number by the Roe-Turkel and HLLC-Turkel methods for the two-phase flow model agrees with the theoretical results inferred for the continuous equations.

This paper is organized as follows. We begin by presenting in Section 2 the two-phase flow model under study. In Section 3 we describe the class of wave propagation schemes and the Riemann solvers that we employ for its numerical solution. Section 4 briefly recalls the fractional step method and the pressure relaxation procedure used for the approximation of the six-equation two-phase system with mechanical relaxation. In Section 5 we highlight some properties of the asymptotic behavior of continuous solutions of the two-phase flow model [28], and we extend the discussion of [12] on the behavior of Roe’s discrete equations and related inaccuracies at low Mach number to discretizations of the six-equation two-phase system. In Section 6 we illustrate in detail our novel preconditioning techniques for the Roe-type and HLLC-type schemes. Numerical results obtained with the proposed preconditioned methods are then presented in Section 7. Some concluding remarks are finally written in Section 8.

## 2. The six-equation two-phase flow model with stiff pressure relaxation

We describe two-phase mixtures evolving in mechanical equilibrium by the six-equation single-velocity two-phase flow model with stiff pressure relaxation first proposed by Saurel and co-workers [2]. Here we adopt the model formulation that we have proposed in [3, 1], which uses the equations for the total energies of the two phases instead of the equations for the phasic internal energies employed in the classical version [2, 41]. The model system has the form:

$$\partial_t \alpha_1 + \vec{u} \cdot \nabla \alpha_1 = \mu (p_1 - p_2), \quad (1a)$$

$$\partial_t (\alpha_1 \rho_1) + \nabla \cdot (\alpha_1 \rho_1 \vec{u}) = 0, \quad (1b)$$

$$\partial_t (\alpha_2 \rho_2) + \nabla \cdot (\alpha_2 \rho_2 \vec{u}) = 0, \quad (1c)$$

$$\partial_t (\rho \vec{u}) + \nabla \cdot (\rho \vec{u} \otimes \vec{u}) + \nabla (\alpha_1 p_1 + \alpha_2 p_2) = 0, \quad (1d)$$

$$\partial_t (\alpha_1 E_1) + \nabla \cdot (\alpha_1 E_1 \vec{u} + \alpha_1 p_1 \vec{u}) + \mathcal{Y}(q, \nabla q) = -\mu p_1 (p_1 - p_2), \quad (1e)$$

$$\partial_t (\alpha_2 E_2) + \nabla \cdot (\alpha_2 E_2 \vec{u} + \alpha_2 p_2 \vec{u}) - \mathcal{Y}(q, \nabla q) = \mu p_1 (p_1 - p_2), \quad (1f)$$

where the non-conservative term  $\mathcal{Y}$  appearing in the phasic total energy equations is

$$\mathcal{Y}(q, \nabla q) = \vec{u} \cdot (Y_1 \nabla (\alpha_2 p_2) - Y_2 \nabla (\alpha_1 p_1)), \quad (1g)$$

with  $q$  denoting the vector of the system unknowns, see equation (3b) below. In the system above  $\alpha_k$  is the volume fraction of phase  $k$ ,  $k = 1, 2$  ( $\alpha_1 + \alpha_2 = 1$ ),  $\rho_k$  is the phasic density,  $p_k$  is the phasic pressure, and  $E_k$  is the phasic total energy,  $E_k = \mathcal{E}_k + \frac{1}{2} \rho_k \vec{u} \cdot \vec{u}$ , where  $\mathcal{E}_k$  is the phasic internal energy per unit volume. The mixture density is  $\rho = \alpha_1 \rho_1 + \alpha_2 \rho_2$ , and  $\vec{u}$  denotes the flow velocity vector. Moreover,  $Y_k = \frac{\alpha_k \rho_k}{\rho}$  denotes the mass fraction of phase  $k$ . The source terms appearing in (1a), (1e), and (1f) model mechanical relaxation. In these terms  $\mu > 0$  represents the pressure relaxation parameter and  $p_1$  is the interface pressure,  $p_1 = \frac{Z_2 p_1 + Z_1 p_2}{Z_1 + Z_2}$ , where  $Z_k = \rho_k c_k$  is the acoustic impedance of phase  $k$ , and  $c_k$  is the sound speed of phase  $k$ . We assume an infinite-rate pressure relaxation with  $\mu \rightarrow +\infty$ , therefore mechanical equilibrium is reached instantaneously. The closure of system (1) is obtained through the specification of an equation of state for each phase, which we choose to express in terms of  $\mathcal{E}_k$  and  $\rho_k$ ,  $p_k = p_k(\mathcal{E}_k, \rho_k)$ ,  $k = 1, 2$ . Here we will restrict our study to the case of species governed by the stiffened gas equation of state (SG EOS), with the following pressure law:  $p_k(\mathcal{E}_k, \rho_k) = (\gamma_k - 1)\mathcal{E}_k - \gamma_k \varpi_k - (\gamma_k - 1)\eta_k \rho_k$ , for  $k = 1, 2$ , where  $\gamma_k$ ,  $\varpi_k$  and  $\eta_k$  are material-dependent parameters. The mixture specific internal energy for the model considered here is defined as  $\varepsilon = Y_1 \varepsilon_1 + Y_2 \varepsilon_2$ , and, equivalently, the mixture internal energy per unit volume is  $\mathcal{E} = \rho \varepsilon = \alpha_1 \mathcal{E}_1 + \alpha_2 \mathcal{E}_2$ . The latter relation, by using the isobaric assumption  $p_1 = p_2 = p$  in the energy laws  $\mathcal{E}_k(p_k, \rho_k)$ ,  $k = 1, 2$ , gives the mixture equation of state, which determines the mixture pressure law  $p = p(\mathcal{E}, \rho_1, \rho_2, \alpha_1)$  by  $\mathcal{E} = \alpha_1 \mathcal{E}_1(p, \rho_1) + \alpha_2 \mathcal{E}_2(p, \rho_2)$ . In the case with the SG EOS this relation gives an explicit expression for the mixture pressure  $p$ . The two-phase model system (1) is hyperbolic, which means that it has real eigenvalues and a complete set of eigenvectors [41, 1]. The eigenvalues are given by  $\lambda_{1,5+d} = \vec{u} \cdot \vec{n} \mp c_f$  and  $\lambda_l = \vec{u} \cdot \vec{n}$  for  $l = 2, \dots, 4 + d$  (eigenvalue of algebraic multiplicity  $3 + d$ ). Here  $c_f$  is the (frozen) mixture sound speed, given by

$$c_f = \sqrt{Y_1 c_1^2 + Y_2 c_2^2}. \quad (2)$$

The phasic sound speed  $c_k$  can be expressed as  $c_k = \sqrt{\kappa_k h_k + \chi_k}$ , where  $\kappa_k = \frac{\partial p_k(\mathcal{E}_k, \rho_k)}{\partial \mathcal{E}_k}$ ,  $\chi_k = \frac{\partial p_k(\mathcal{E}_k, \rho_k)}{\partial \rho_k}$ , and  $h_k = \frac{\mathcal{E}_k + p_k}{\rho_k}$  is the phasic specific enthalpy,  $k = 1, 2$ . For the stiffened gas EOS, we have  $\kappa_k = (\gamma_k - 1)$  and  $\chi_k = -(\gamma_k - 1)\eta_k$ . System (1) can be written in a compact form as

$$\partial_t q + \nabla \cdot \mathcal{F}(q) + \zeta(q, \nabla q) = \psi(q), \quad (3a)$$

$$\text{where } q = [\alpha_1, \alpha_1 \rho_1, \alpha_2 \rho_2, \rho \vec{u}, \alpha_1 E_1, \alpha_2 E_2]^\top, \quad (3b)$$

$$\mathcal{F}(q) = [0, \alpha_1 \rho_1 \vec{u}, \alpha_2 \rho_2 \vec{u}, \rho \vec{u} \otimes \vec{u} + (\alpha_1 p_1 + \alpha_2 p_2) \mathbb{I}, \alpha_1 (E_1 + p_1) \vec{u}, \alpha_2 (E_2 + p_2) \vec{u}]^\top, \quad (3c)$$

$$\zeta(q, \nabla q) = [\vec{u} \cdot \nabla \alpha_1, 0, 0, 0, \mathcal{Y}(q, \nabla q), -\mathcal{Y}(q, \nabla q)]^\top, \quad (3d)$$

$$\psi(q) = [\mu(p_1 - p_2), 0, 0, 0 - \mu p_1(p_1 - p_2), \mu p_1(p_1 - p_2)]^\top, \quad (3e)$$

with  $\mathcal{Y}$  as in (1g). Above we have put into evidence the conservative portion of the spatial derivative contributions in the system as  $\nabla \cdot \mathcal{F}(q)$ , and we have indicated the non-conservative term as  $\zeta(q, \nabla q)$ . The source term  $\psi(q)$  contains mechanical relaxation terms. Let us also note that the sum of the two equations for the phasic total energies (1e), (1f) recovers the conservation law for the mixture total energy  $E = \alpha_1 E_1 + \alpha_2 E_2$ :  $\partial_t E + \nabla \cdot (E \vec{u} + (\alpha_1 p_1 + \alpha_2 p_2) \vec{u}) = 0$ .

### 2.1. The limit five-equation pressure equilibrium two-phase flow model

In the instantaneous pressure relaxation limit the six-equation model (1) is equivalent to the five-equation single-velocity single-pressure two-phase flow model of Kapila *et al.* [5], see [2]. By adopting a nomenclature analogous to the one introduced for the six-equation model in the previous section, and denoting here with  $p$  and  $E$  the equilibrium pressure and total energy of the mixture, respectively, this model has the form:

$$\partial_t \alpha_1 + \vec{u} \cdot \nabla \alpha_1 = \alpha_1 \alpha_2 \frac{\rho_2 c_2^2 - \rho_1 c_1^2}{\alpha_2 \rho_1 c_1^2 + \alpha_1 \rho_2 c_2^2} \nabla \cdot \vec{u}, \quad (4a)$$

$$\partial_t (\alpha_1 \rho_1) + \nabla \cdot (\alpha_1 \rho_1 \vec{u}) = 0, \quad (4b)$$

$$\partial_t (\alpha_2 \rho_2) + \nabla \cdot (\alpha_2 \rho_2 \vec{u}) = 0, \quad (4c)$$

$$\partial_t (\rho \vec{u}) + \nabla \cdot (\rho \vec{u} \otimes \vec{u}) + \nabla p = 0, \quad (4d)$$

$$\partial_t E + \nabla \cdot ((E + p) \vec{u}) = 0. \quad (4e)$$

This 5-equation model is hyperbolic with eigenvalues  $\lambda_{1,4+d} = \vec{u} \cdot \vec{n} \mp c_W$  and  $\lambda_l = \vec{u} \cdot \vec{n}$  for  $l = 2, \dots, 3 + d$ . The speed of sound  $c_W$  here corresponds to the Wood's mixture equilibrium sound speed [42] defined by

$$c_W = \sqrt{\frac{1}{\rho} \left( \frac{\alpha_1}{\rho_1 c_1^2} + \frac{\alpha_2}{\rho_2 c_2^2} \right)^{-1}}. \quad (5)$$

Note that  $c_W \leq c_f$ , which expresses Liu's sub-characteristic condition for the pressure-relaxed system. The behavior of the frozen sound speed  $c_f$  and Wood's sound speed  $c_W$  versus the volume fraction can be observed in the example in Figure 1 for a liquid-vapor water mixture. Let us remark that the 5-equation equilibrium model represents the physical flow model that we are approximating by solving the six-equation model (1) with instantaneous mechanical equilibrium  $\mu \rightarrow +\infty$ . Solving the 6-equation system with  $\mu \rightarrow +\infty$  instead of the 5-equation equilibrium system offers numerically several advantages, cf. [2, 1]. The main numerical issues in the solution of the 5-equation system come from the non-conservative contribution in the volume fraction equation that depends on the divergence of the flow velocity.

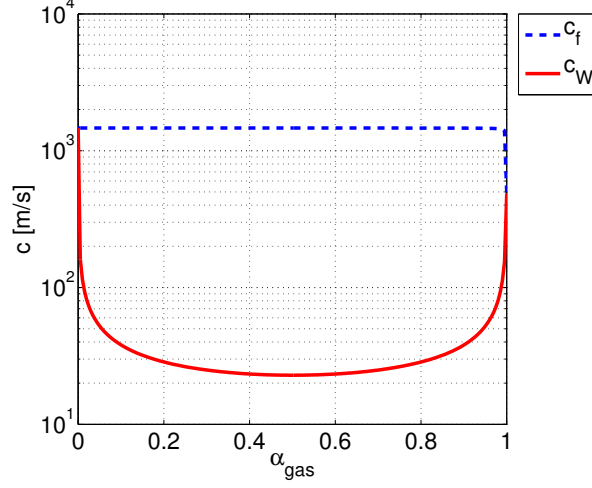


Figure 1: Semi-logarithmic graph of the frozen mixture sound speed  $c_f$  (sound speed of the homogeneous 6-equation model) and Wood's sound speed  $c_W$  (sound speed of the pressure-equilibrium 5-equation model) versus the gaseous phase volume fraction for a liquid-vapor water mixture. Pressure and temperature are fixed to  $p = 10^5$  Pa and  $T = 373$  K. Here we adopt the stiffened gas EOS with the parameters used in the numerical experiments in Section 7.

### 3. Wave propagation schemes

To numerically solve the the 6-equation two-phase flow model (1) with no source term ( $\psi = 0$ ) we use the finite volume wave propagation schemes of LeVeque [43, 44, 45]. These schemes are a class of Godunov-type methods based on Riemann solvers [46] to approximate hyperbolic systems of partial differential equations. In the two-dimensional case we consider the solution of hyperbolic systems of the form  $\partial_t q + A(q)\partial_x q + B(q)\partial_y q = 0$ , with  $q \in \mathbb{R}^N$  and  $A(q), B(q) \in \mathbb{R}^{N \times N}$ . We focus here on the spatial discretization. We assume a Cartesian grid with cells of uniform size  $\Delta x$  and  $\Delta y$  in the  $x$  and  $y$  directions, respectively. We denote by  $q_{i,j}$  the approximate solution of the system at the cell  $(i, j)$  corresponding to  $[x_{i-1/2}, x_{i+1/2}] \times [y_{j-1/2}, y_{j+1/2}]$ ,  $i, j \in \mathbb{Z}$ . The two-dimensional first order wave propagation algorithm has the semi-discrete form

$$\frac{dq_{i,j}}{dt} + \frac{1}{\Delta x} (\mathcal{A}^+ \Delta Q_{i-1/2,j} + \mathcal{A}^- \Delta Q_{i+1/2,j}) + \frac{1}{\Delta y} (\mathcal{B}^+ \Delta Q_{i,j-1/2} + \mathcal{B}^- \Delta Q_{i,j+1/2}) = 0. \quad (6)$$

Here  $\mathcal{A}^\pm \Delta Q$  and  $\mathcal{B}^\pm \Delta Q$  are the fluctuations arising from plane-wave Riemann problems at cell interfaces in the  $x$  and  $y$  directions [43]. That is, the fluctuations  $\mathcal{A}^\pm \Delta Q_{i+1/2,j}$  are obtained by solving Riemann problems for the system  $\partial_t q + A(q)\partial_x q = 0$  at interfaces  $x_{i+1/2}$ , and the fluctuations  $\mathcal{B}^\pm \Delta Q_{i,j+1/2}$  are obtained by solving Riemann problems for  $\partial_t q + B(q)\partial_y q = 0$  at interfaces  $y_{j+1/2}$ . The first order scheme (6) can be extended to formal second order accuracy by adding suitable correction terms [43, 44]. However, here we are interested in studying the performance of simple first-order schemes. The method (6) above can be generalized in a straightforward manner to logically rectangular quadrilateral grids (curvilinear grids) to perform computations in irregularly-shaped domains, see [44, 43].

### 3.1. Approximate Riemann solvers

To compute the fluctuations  $\mathcal{A}^\pm \Delta Q$  and  $\mathcal{B}^\pm \Delta Q$  in (6) a Riemann solver (cf. [46, 44]) must be provided. We consider here the approximation of a two-dimensional plane-wave Riemann problem in the  $x$  direction for the homogeneous 6-equation two-phase flow model (1), hence the Riemann solution to a one-dimensional system of  $N = 7$  equations of the form

$$\partial_t q + \partial_x f(q) + \zeta(q, \partial_x q) = 0, \quad (7a)$$

$$q = [\alpha_1, \alpha_1 \rho_1, \alpha_2 \rho_2, \rho u, \rho v, \alpha_1 E_1, \alpha_2 E_2]^\top, \quad (7b)$$

$$f(q) = [0, \alpha_1 \rho_1 u, \alpha_2 \rho_2 u, \rho u^2 + \alpha_1 p_1 + \alpha_2 p_2, \rho u v, \alpha_1 (E_1 + p_1) u, \alpha_2 (E_2 + p_2) u], \quad (7c)$$

$$\zeta(q, \partial_x q) = [u \partial_x \alpha_1, 0, 0, 0, 0, \Upsilon(q, \partial_x q), -\Upsilon(q, \partial_x q)]^\top, \quad (7d)$$

where  $\Upsilon(q, \partial_x) = u(Y_1 \partial_x (\alpha_2 p_2) - Y_2 \partial_x (\alpha_1 p_1))$ , and where  $u$  and  $v$  denote the velocity components in the  $x$  and  $y$  directions, respectively. Moreover, the associated equation for the mixture total energy is  $\partial_t E + \partial_x f^E(q) = 0$ , where  $f^E = f^{(6)} + f^{(7)} = (E + (\alpha_1 p_1 + \alpha_2 p_2))u$  is the associated flux function. The case of a plane-wave Riemann problem in the  $y$  direction is analogous, except that the roles of  $u$  and  $v$  are inverted and the components of the  $x$  and  $y$  momentum fluxes in  $f$  are switched. Let us consider a Riemann problem with left and right initial data  $q_\ell = q_{i,j}$  and  $q_r = q_{i+1,j}$ , respectively. For simplicity in the following we will omit subscripts  $j$  associated to the grid discretization in the  $y$  direction. The solution structure defined by a Riemann solver can be expressed in general by a set of  $\mathcal{M}$  waves  $\mathcal{W}^l$  and corresponding speeds  $s^l$ ,  $\mathcal{M} \gtrless N$ . The sum of the waves  $\mathcal{W}^l$  must be equal to the initial jump in the vector  $q$  of the system variables:

$$\Delta q \equiv q_r - q_\ell = \sum_{l=1}^{\mathcal{M}} \mathcal{W}^l. \quad (8)$$

Moreover, for the variables  $q^{(\xi)}$ ,  $\xi = 2, 3, 4, 5$  of the flow model governed by conservative equations, namely the partial densities  $\alpha_k \rho_k$  and the mixture momentum components  $\rho u$ ,  $\rho v$ , the initial jump in the flux function  $f^{(\xi)}$  associated to  $q^{(\xi)}$  must be recovered by the sum of the associated wave components multiplied by the corresponding wave speeds:

$$\Delta f^{(\xi)} \equiv f^{(\xi)}(q_r) - f^{(\xi)}(q_\ell) = \sum_{l=1}^{\mathcal{M}} s^l \mathcal{W}^{l(\xi)}, \quad (9)$$

where  $\mathcal{W}^{l(\xi)}$  denotes the  $\xi$ th component of the  $l$ th wave,  $l = 1, \dots, \mathcal{M}$ . The following additional condition must be fulfilled for conservation of the mixture total energy  $E$ :

$$\Delta f^E \equiv f^E(q_r) - f^E(q_\ell) = \sum_{l=1}^{\mathcal{M}} s^l (\mathcal{W}^{l(6)} + \mathcal{W}^{l(7)}). \quad (10)$$

Once the Riemann solution structure  $\{\mathcal{W}_{i+1/2}^l, s_{i+1/2}^l\}_{l=1, \dots, \mathcal{M}}$  arising at each cell edge  $x_{i+1/2}$  is defined through a Riemann solver, the fluctuations  $\mathcal{A}^\pm \Delta Q_{i+1/2}$  to be used in (6) are computed as

$$\mathcal{A}^\pm \Delta Q_{i+1/2} = \sum_{l=1}^{\mathcal{M}} (s_{i+1/2}^l)^\pm \mathcal{W}_{i+1/2}^l, \quad (11)$$

where  $s^+ = \max(s, 0)$  and  $s^- = \min(s, 0)$ . Since in order to apply low Mach number preconditioning techniques to our schemes we need to make explicit the numerical viscosity contribution that is corrected at low Mach number we here rewrite the standard definition above of the fluctuations (11) in a suitable viscous form:

$$\mathcal{A}^\pm \Delta Q_{i+1/2} = \frac{1}{2} \Delta \tilde{f}_{i+1/2} \pm \frac{1}{2} \mathcal{V} \Delta Q_{i+1/2}, \quad (12)$$

where

$$\Delta \tilde{f}_{i+1/2} \equiv \sum_{l=1}^{\mathcal{M}} s_{i+1/2}^l \mathcal{W}_{i+1/2}^l, \quad (13)$$

and the dissipation term  $\mathcal{V} \Delta Q_{i+1/2}$  is given by

$$\mathcal{V} \Delta Q_{i+1/2} = \sum_{l=1}^{\mathcal{M}} |s_{i+1/2}^l| \mathcal{W}_{i+1/2}^l. \quad (14)$$

For many schemes one can write  $\mathcal{V} \Delta Q_{i+1/2} = \Theta_{i+1/2} (q_{i+1} - q_i)$ , where  $\Theta_{i+1/2}$  is the numerical dissipation matrix (viscosity matrix). Let us also remark that for conserved quantities associated to a flux function  $f$  we have  $\Delta \tilde{f}_{i+1/2} = \Delta f_{i+1/2} = f(q_{i+1}) - f(q_i)$ .

### 3.1.1. Roe-type Riemann solver

The idea of the celebrated Roe's Riemann solver originally introduced for the Euler equations [47] is to define an approximate solution to a Riemann problem for a nonlinear hyperbolic system of the form  $\partial_t q + A(q) \partial_x q = 0$  by the exact solution of a Riemann problem for a linearized system  $\partial_t q + \hat{A}(q_\ell, q_r) \partial_x q = 0$ . The constant coefficient matrix  $\hat{A} = \hat{A}(q_\ell, q_r)$  (Roe matrix) is defined locally by evaluating the matrix  $A(q)$  of the original system written in quasi-linear form at a suitable average state between  $q_\ell$  and  $q_r$ . This average state must be chosen so that the Roe matrix satisfies conservation consistency relations. In [1] we have applied this approach to our 6-equation two-phase system. In this case the Roe matrix is defined to fulfill the conservation conditions (9) and (10). The Riemann solution structure of the Roe solver consists of  $\mathcal{M} = N = 7$  waves and speeds that correspond to the eigenstructure of the Roe matrix. Denoting with  $\hat{r}_l$  and  $\hat{\lambda}_l$  the right eigenvectors and eigenvalues of  $\hat{A}$ , respectively, we have

$$\mathcal{W}^l = \hat{\zeta}_l \hat{r}_l \quad \text{and} \quad s^l = \hat{\lambda}_l, \quad l = 1, \dots, 7, \quad (15)$$

where  $\hat{\zeta}_l$  are the coefficients of the projection of the jump  $q_r - q_\ell$  onto the basis of the Roe eigenvectors,  $q_r - q_\ell = \sum_{l=1}^7 \hat{\zeta}_l \hat{r}_l$ . The definition of the Roe eigenstructure for the two-phase flow model for the case of the stiffened gas EOS is reported in Appendix A. Considering here  $q_\ell = q_i$ ,  $q_r = q_{i+1}$ , and denoting  $\hat{A}_{i+1/2} = \hat{A}(q_i, q_{i+1})$ , we can then write the numerical dissipation term (14) of our Roe-type scheme as

$$\mathcal{V} \Delta Q_{i+1/2} = \sum_{l=1}^7 (|\hat{\lambda}_l| \hat{\zeta}_l \hat{r}_l)_{i+1/2} = \hat{R}_{i+1/2} |\hat{\Lambda}_{i+1/2}| \hat{R}_{i+1/2}^{-1} (q_{i+1} - q_i) = |\hat{A}_{i+1/2}| (q_{i+1} - q_i), \quad (16)$$

where  $\hat{R} = [\hat{r}_1 \dots \hat{r}_7]$  and  $\hat{\Lambda} = \text{diag}(\hat{\lambda}_1, \dots, \hat{\lambda}_7)$ . The numerical viscosity matrix of the Roe-type scheme is then identified as  $\Theta_{i+1/2} = |\hat{A}_{i+1/2}|$ , analogously to the single-phase case [12].

### 3.1.2. HLLC-type Riemann solver in a novel form

Although efficient for a large variety of problems, the Roe-type solver might suffer in some situations from the appearance of non-physical states, such as non-positive densities and/or non-positive energies. This has motivated us to develop in [1] an HLLC-type Riemann solver [48, 46] for the 6-equation model (1). This HLLC-type solver is much more robust than the Roe-type solver, especially when heat and mass transfer processes are included in the two-phase flow model. Our scheme consists in applying the standard HLLC method [48, 46] to the conservative portion of the two-phase system. Although discretizations of the non-conservative terms in the energy equations can be included, we choose the simplest method that neglects the  $\pm \mathcal{Y}$  terms. We refer to [1] for a discussion on this point and the rationale for this approach. In general the HLLC Riemann solution consists of three waves  $\mathcal{W}^l$ ,  $l = 1, 2, 3$ , moving at speeds

$$s^1 = S^\ell, \quad s^2 = S^*, \quad \text{and} \quad s^3 = S^r, \quad (17)$$

which separate four constant states  $q_\ell$ ,  $q^{*\ell}$ ,  $q^{*r}$  and  $q_r$ . In the following we will indicate with  $(\cdot)^{*\ell}$  and  $(\cdot)^{*r}$  quantities corresponding to the states  $q^{*\ell}$  and  $q^{*r}$  adjacent, respectively on the left and on the right, to the middle wave propagating at speed  $S^*$ . With this notation, the waves of the HLLC solver are  $\mathcal{W}^1 = q^{*\ell} - q_\ell$ ,  $\mathcal{W}^2 = q^{*r} - q^{*\ell}$ ,  $\mathcal{W}^3 = q_r - q^{*r}$ . These waves and speeds must satisfy the conservation conditions (9), (10). Moreover, since here we neglect non-conservative terms in the phasic energy equations, we also impose relations of the form (9) for  $\xi = 6, 7$ , that is for the conservative portion of the equations for  $\alpha_k E_k$ . Since  $f^E(q) = f^{(6)}(q) + f^{(7)}(q)$ , this clearly guarantees conservation of the mixture total energy (eq. (10)). The speed  $S^*$  is determined as in [46]. The middle states  $q^{*\ell}$ ,  $q^{*r}$  are found as:

$$q^{*\iota} = \begin{pmatrix} \alpha_{1,\iota} \\ (\alpha_k \rho_k)_\iota \frac{S^\iota - u_\iota}{S^\iota - S^*} \quad k = 1, 2 \\ \rho_\iota \frac{S^\iota - u_\iota}{S^\iota - S^*} S^* \\ \rho_\iota \frac{S^\iota - u_\iota}{S^\iota - S^*} v_\iota \\ (\alpha_k \rho_k)_\iota \frac{S^\iota - u_\iota}{S^\iota - S^*} \left( \frac{E_{k,\iota}}{\rho_{k,\iota}} + (S^* - u_\iota) \left( S^* + \frac{p_{k,\iota}}{\rho_{k,\iota}(S^\iota - u_\iota)} \right) \right) \quad k = 1, 2 \end{pmatrix}, \quad (18)$$

$\iota = \ell, r$ . Here we now present a novel reformulation of the acoustic waves  $\mathcal{W}^{1,3}$  of the HLLC solver in order to be able to extend to our HLLC-type method the low Mach number preconditioning techniques conceived for the Roe's solver [12]. This will be illustrated for the HLLC solver for the Euler equations in a separate work. First we introduce two quantities  $\check{c}^\ell$ ,  $\check{c}^r$  representing the speeds of sound associated to the external acoustic waves by defining:

$$S^\ell = u_\ell - \check{c}^\ell \quad \text{and} \quad S^r = u_r + \check{c}^r. \quad (19)$$

The speed  $S^*$  can be written in terms of  $\check{c}^\ell$  and  $\check{c}^r$  as:

$$S^* = \frac{\Delta p_m + \rho_\ell u_\ell (S^\ell - u_\ell) - \rho_r u_r (S^r - u_r)}{\rho_\ell (S^\ell - u_\ell) - \rho_r (S^r - u_r)} = \frac{\rho_\ell \check{c}^\ell u_\ell + \rho_r \check{c}^r u_r - \Delta p_m}{\rho_\ell \check{c}^\ell + \rho_r \check{c}^r}, \quad (20)$$

where  $p_m = \alpha_1 p_1 + \alpha_2 p_2$ . The densities  $\rho^{*\iota}$ ,  $\iota = \ell, r$ , corresponding to the middle states can be expressed as

$$\rho^{*\ell} = \rho_\ell \frac{\check{c}^\ell}{S^* - u_\ell + \check{c}^\ell} \quad \text{and} \quad \rho^{*r} = \rho_r \frac{\check{c}^r}{u_r - S^* + \check{c}^r}. \quad (21)$$

Then, after some manipulations, we easily see that the acoustic waves of the HLLC-type solver for the 6-equation two phase flow model can be equivalently written in a form that reveals the mathematical analogy with the waves of the Roe-type solver (see Appendix A). We have

$$\mathcal{W}^{1,3} = \check{\zeta}_{1,3} \check{r}_{1,3}, \quad \check{r}_1 = \begin{pmatrix} 0 \\ Y_{1,\ell} \\ Y_{2,\ell} \\ u_\ell - \check{c}^\ell \\ v_\ell \\ Y_{1,\ell}(H_{1,\ell} - S^* \check{c}^\ell) \\ Y_{2,\ell}(H_{2,\ell} - S^* \check{c}^\ell) \end{pmatrix}, \quad \check{r}_3 = \begin{pmatrix} 0 \\ Y_{1,r} \\ Y_{2,r} \\ u_r + \check{c}^r \\ v_r \\ Y_{1,r}(H_{1,r} + S^* \check{c}^r) \\ Y_{2,r}(H_{2,r} + S^* \check{c}^r) \end{pmatrix}, \quad (22a)$$

$$\check{\zeta}_1 = \frac{\rho^{*\ell}}{\rho_\ell \check{c}^\ell + \rho_r \check{c}^r} \left( \frac{\Delta p_m}{\check{c}^\ell} - \rho_r \frac{\check{c}^r}{\check{c}^\ell} \Delta u \right), \quad \check{\zeta}_3 = \frac{\rho^{*r}}{\rho_\ell \check{c}^\ell + \rho_r \check{c}^r} \left( \frac{\Delta p_m}{\check{c}^r} + \rho_\ell \frac{\check{c}^\ell}{\check{c}^r} \Delta u \right). \quad (22b)$$

In these expressions the sound speed  $\check{c}$  corresponds to the mixture sound speed (2). Finally, a definition for the wave speeds  $S^\ell, S^r$  must be provided. Here we adopt the definition proposed by Davis [49]:  $S^\ell = \min(u_\ell - c_\ell, u_r - c_r)$ ,  $S^r = \max(u_\ell + c_\ell, u_r + c_r)$ , which implies:

$$\check{c}^\ell = \max(c_\ell, c_r + u_\ell - u_r) \quad \text{and} \quad \check{c}^r = \max(c_r, c_\ell + u_\ell - u_r). \quad (23)$$

### 3.2. Temporal integration

Since, as explained in the Introduction, the present work focuses on the loss of accuracy at low Mach number related to the spatial discretization of the convective portion of the model equations, here we use a standard explicit method for the time integration of (6). Denoting with  $\Delta t$  the time step and with  $Q_{ij}^n$  the the approximate solution at the cell  $(i, j)$  at time  $t^n$ ,  $i, j \in \mathbb{Z}$ ,  $n \in \mathbb{N}$ , the fully discrete first-order two-dimensional scheme has the form [44, 43]

$$Q_{ij}^{n+1} = Q_{ij}^n - \frac{\Delta t}{\Delta x} \left( \mathcal{A}^+ \Delta Q_{i-1/2,j}^n + \mathcal{A}^- \Delta Q_{i+1/2,j}^n \right) - \frac{\Delta t}{\Delta y} \left( \mathcal{B}^+ \Delta Q_{i,j-1/2}^n + \mathcal{B}^- \Delta Q_{i,j+1/2}^n \right). \quad (24)$$

For low Mach number flows the Courant–Friedrichs–Lewy (CFL) condition for this time-explicit scheme requires a very small time step  $\Delta t = \mathcal{O}(M)$  as  $M \rightarrow 0$ . Moreover, when preconditioning is activated, the stability condition on the time step is much more severe, and a time step  $\Delta t = \mathcal{O}(M^2)$  is needed, see the analysis of Birken–Meister in [36]. Therefore, as mentioned in the Introduction, the current method remains computationally very expensive for very small Mach numbers, a difficulty that we plan to address in future work by adopting implicit time integration.

## 4. Numerical solution of the two-phase flow model system with mechanical relaxation

To numerically solve the two-phase flow model system (3) with stiff mechanical relaxation we use a fractional step technique, where we alternate between the solution of the homogeneous hyperbolic system  $\partial_t q + \nabla \cdot \mathcal{F}(q) + \zeta(q, \nabla q) = 0$  and the solution of a system of ordinary differential equations that takes into account the pressure relaxation source term  $\psi(q)$ :  $\partial_t q = \psi(q)$ . The homogeneous system is solved by the wave propagation method described in Section 3 by using either the Roe-type solver or the HLLC-type solver. The system of ordinary differential equations  $\partial_t q = \psi(q)$  is solved in the limit of instantaneous relaxation  $\mu \rightarrow +\infty$ , by employing the procedure that we have presented in [1]. Let us denote with superscript 0 the quantities coming

from the solution of the homogeneous system, and with superscript  $\oplus$  the quantities representing the solution at mechanical equilibrium. It is easy to observe that the system  $\partial_t q = \psi(q)$  implies  $(\alpha_k \rho_k)^\oplus = (\alpha_k \rho_k)^0$ ,  $k = 1, 2$ , and  $(\rho \vec{u})^\oplus = (\rho \vec{u})^0$ , this yielding also  $\rho^\oplus = \rho^0$  and  $\vec{u}^\oplus = \vec{u}^0$ . Moreover we note that the sum of the phasic energy equations gives  $\partial_t E = \partial_t \mathcal{E} = 0$ , and hence  $E^\oplus = E^0$  and  $\mathcal{E}^\oplus = \mathcal{E}^0$ , meaning that the total energy and the internal energy of the two-phase mixture do not vary as the phasic pressures relax toward the equilibrium value  $p^\oplus$ . By approximating the interface pressure  $p_1$  by a convex average constant in time  $\bar{p}_1 = (1-\theta)p_1^0 + \theta p^\oplus$ ,  $\theta \in [0, 1]$ , the two differential phasic energy equations can be easily integrated, and we obtain

$$(\alpha_k E_k)^\oplus - (\alpha_k E_k)^0 = (\alpha_k \mathcal{E}_k)^\oplus - (\alpha_k \mathcal{E}_k)^0 = (-1)^k \frac{\bar{p}_1}{2} (\alpha_1^\oplus - \alpha_1^0), \quad k = 1, 2. \quad (25)$$

In [1] we chose  $\theta = 1/2$ , hence  $\bar{p}_1 = \frac{p_1^0 + p_1^\oplus}{2}$ , which is equivalent to assume a linear variation of the interface pressure  $p_1$  with  $\alpha_1$ . An alternative choice, used in the present work, is  $\theta = 1$ , hence  $\bar{p}_1 = p^\oplus$ . Based on our experience and the observations in [2], no relevant differences are observed in the numerical results obtained with these two choices of  $\theta$ . Next, we impose mechanical equilibrium at final time:  $p_1^\oplus = p_2^\oplus = p_1^\oplus = p^\oplus$ . The phasic internal energies are hence expressed by  $\mathcal{E}_k^\oplus = \mathcal{E}_k(p^\oplus, (\alpha_k \rho_k)^0 / \alpha_k^\oplus)$  for  $k = 1, 2$ . With these relations system (25) gives two equations for the two unknowns  $\alpha_1^\oplus$  and  $p^\oplus$ . For the particular case of the SG EOS we can obtain a simple quadratic equation for the relaxed pressure  $p^\oplus$  and then we easily compute the relaxed volume fraction  $\alpha_1^\oplus$ .

## 5. The continuous and the discrete two-phase flow model in the low Mach number limit

To better understand the difficulties encountered by upwind finite volume methods at low Mach number it is useful to analyze the considered flow model in the low Mach number limit both at the continuous and at the discrete level. Since the physical flow model that we approximate by solving the six-equation two-phase flow model with instantaneous mechanical relaxation corresponds to the reduced five-equation pressure equilibrium two-phase flow model (4) of Kapila *et al.* [5], we are interested in the asymptotic behavior in the low Mach number limit of the latter model at the continuous level. The low Mach number behavior of the 5-equation model was first studied by Murrone and Guillard in [28], by using a classical asymptotic expansion approach (e.g. [12, 18, 7]). We briefly recall here the relevant points of [28]. One starts by writing system (4) in non-dimensionalized form, by using the non-dimensionalized variables  $\alpha'_1 = \alpha_1$ ,  $\rho'_k = \frac{\rho_k}{\rho_*}$ ,  $\vec{u}' = \frac{\vec{u}}{u_*}$ ,  $p' = \frac{p}{\rho_* c_{W*}^2}$ ,  $\vec{x}' = \frac{\vec{x}}{x_*}$ ,  $t' = \frac{t u_*}{x_*}$ , where  $x_*$  is a length scale, the subscript  $*$  denotes reference quantities, and  $u_* = \max_{\vec{x} \in \Omega} v(\vec{x}, 0)$  for any flow variable  $v(\vec{x}, t)$  in the considered bounded domain  $\Omega$ . A reference Mach number  $M_{W*}$  is defined based on the equilibrium speed of sound  $c_W$  (5),  $M_{W*} = \frac{u_*}{c_{W*}}$ . Then, we assume single scale asymptotic expansions of the system's variables of the form

$$(\cdot) = (\cdot)^{[0]} + (\cdot)^{[1]} M_{W*} + (\cdot)^{[2]} M_{W*}^2 + \dots \quad (26)$$

This Ansatz of single time scale and single space scale representation means that we do not allow for high-frequency acoustics and long wave length acoustics, which can be accounted for via a multi scale asymptotic analysis [50, 51, 22]. For consistency, *well prepared* initial conditions are also assumed [7], which means that initially the pressure is uniform except for perturbations of order  $O(M^2)$  and the flow field is divergence-free except for perturbations of order  $O(M)$ ,  $M \rightarrow 0$ . The investigation of solutions within a single scale analysis is of particular interest here since it

provides insight into some of the reasons of the failure of conventional upwind schemes in the low Mach number limit, as discussed hereafter. From a physical point of view, the considered regime is relevant in several application problems of interest such as steady cavitating flows in nozzles or around hydrofoils. Introducing the expansions (26) in the system's equations and collecting terms with the same order in  $M_{W*}$ , one obtains  $\nabla \dot{p}^{[0]} = 0$  and  $\nabla \dot{p}^{[1]} = 0$ , hence  $\dot{p}^{[0]}$  and  $\dot{p}^{[1]}$  are functions of time only. We will omit in the sequel the acute accent denoting non-dimensionalized variables. Therefore we infer, in complete analogy with the case of the Euler equations, that in the low Mach number limit the pressure can be written as a constant in space up to fluctuations of order  $M_{W*}^2$  [28]:

$$p(\vec{x}, t) = \mathcal{P}^{[0]}(t) + p^{[2]}(\vec{x}, t)M_{W*}^2 + \dots \quad (27)$$

Here the first-order spatially constant pressure term  $p^{[1]}$  has been integrated in the leading order pressure term denoted with  $\mathcal{P}^{[0]}$ . This is based on the fact that zeroth-order components and sums of zeroth-order and first-order components (e.g.  $p^{[0]} + M_* p^{[1]}$ ) satisfy equations of the same form [51, 52, 53] within a single scale analysis, and there is no need to consider the  $p^{[1]}$  term separately. The temporal change of the leading order pressure is due to compression or expansion at the boundaries. In the presence of open boundaries with a constant exterior pressure  $p_0$  we simply have  $\mathcal{P}^{[0]} = p_0$ . The result in (27) characterizes the low Mach number limit of the 5-equation model as well as the limit of the 6-equation model with instantaneous pressure relaxation as the Mach number of the equilibrium mixture goes to zero. Note that, assuming constant pressure at open boundaries and further assuming that at open boundaries and initially the volume fraction is equal to a constant  $\alpha_{1,0}$  (in other words, particle paths come from regions with constant volume fraction), we can deduce from the volume fraction and pressure equations that in the low Mach number limit the volume fraction is equal to  $\alpha_{1,0}$  up to fluctuations of order  $M_{W*}^2$ .

Although the continuous 6-equation two-phase flow model of physical interest is the one with mechanical relaxation, it is useful to make some observations on the behavior in the low Mach number limit of the continuous homogeneous 6-equation model ( $\psi = 0$ ). This can provide a better understanding of the difficulties encountered at low Mach number at the discrete level, since our numerical method based on the fractional step algorithm described in Section 4 employs solutions of the homogeneous system. We consider the non-dimensionalized form of the homogeneous 6-equation model (1), by using analogous non-dimensional variables as for the 5-equation model, except that here the reference sound speed corresponds to the frozen sound speed  $c_f$  (2) and the reference Mach number is based on this non-equilibrium sound speed,  $M_{f*} = \frac{u_*}{c_{f*}}$ . In particular, we can write the following non-dimensionalized equations for the velocity and the effective pressure  $p_m = \alpha_1 p_1 + \alpha_2 p_2$ :  $\rho(\partial_t \vec{u} + (\vec{u} \cdot \nabla) \vec{u}) + \nabla p_m / M_{f*}^2 = 0$  and  $\partial_t p_m + \vec{u} \cdot \nabla p_m + \rho c_f^2 \nabla \cdot \vec{u} = 0$ , which are analogous to the non-dimensional equations inferred for the velocity  $\vec{u}$  and the pressure  $p$  of the Euler system, see e.g. [12, 18]. By using again asymptotic expansions of the variables in terms of powers of  $M_{f*}$  similar to (26), one finds at order  $M_{f*}^{-2}$  and  $M_{f*}^{-1}$  that  $\nabla p_m^{[0]} = 0$  and  $\nabla p_m^{[1]} = 0$ , respectively. Therefore we can write:

$$p_m(\vec{x}, t) = \mathcal{P}_m^{[0]}(t) + p_m^{[2]}(\vec{x}, t)M_{f*}^2 + \dots \quad (28)$$

as  $M_{f*} \rightarrow 0$ . As expected, the results of the asymptotic analysis are analogous to the single-phase case, except that here the effective pressure  $p_m$  plays the role of  $p$  in the Euler equations. Let us recall that the frozen sound speed  $c_f$  satisfies the sub-characteristic condition  $c_W \leq c_f$ , therefore  $M_{f*} = \frac{c_{W*}}{c_{f*}} M_{W*} \leq M_{W*}$ . Hence, the hypothesis of low Mach number for the equilibrium model

entails low Mach number regimes for the non-equilibrium model, and, moreover, terms of order  $M_{f*}^\phi$  are bounded by quantities of order  $M_{W*}^\phi$ ,  $\phi \in \mathbb{N}$ .

### 5.1. Discrete two-phase equations

Similar to the well known case of the single-phase Euler equations [8, 12, 18, 31], discrete solutions of the 5-equation two-phase flow model computed by upwind finite volume methods are not accurate approximations of solutions of the continuous model for vanishing Mach number. These difficulties arise both for numerical methods based on direct discretizations of the 5-equation model [28] and for schemes based on approximations of the 6-equation model with stiff mechanical relaxation ( $\mu \rightarrow +\infty$ ) as in our case (see also [30]). This issue can be better understood by studying the behavior at low Mach number of the discrete equations by an asymptotic analysis similar to the one illustrated above for the continuous model. This has been done for the Roe's scheme for the classical Euler system in [12]. We briefly present here the analysis for our Roe-type method for the 6-equation two-phase flow model, by analyzing the two-dimensional semi-discrete equations (24) on a Cartesian grid. For simplicity we assume  $\Delta x = \Delta y \equiv \delta$ . To write the discrete equations in a more compact form as in [12] we use the index  $J = (i, j)$  to indicate the grid cell  $(i, j)$ , and we introduce the index set for neighboring cells  $v(J) = \{(i-1, j), (i+1, j), (i, j-1), (i, j+1)\}$ . Moreover, we define the jump operator  $\Delta_{JK}(\cdot) \equiv (\cdot)_J - (\cdot)_K$  that expresses the difference between values at the reference cell  $J$  and its neighboring cell  $K$ , and we denote with  $(\cdot)_{JK}$  quantities corresponding to interfaces between cells  $J$  and  $K$ . In particular, we will denote with  $\hat{(\cdot)}_{JK}$  Roe-averaged quantities at the interface  $JK$ . We use  $\vec{n}_{JK} = (n_x, n_y)_{JK}$  to denote the unit normal vector to the interface  $JK$ , from cell  $J$  to cell  $K$ , and the transverse unit vector is then  $\vec{n}_{JK}^\perp = (-n_y, n_x)_{JK}$ . We indicate the normal and transverse components of  $\vec{u} = (u, v)$  with  $U = \vec{u} \cdot \vec{n}$  and  $V = \vec{u} \cdot \vec{n}^\perp$ , respectively. The non-dimensionalized semi-discrete equations for the first order Roe-type scheme for the 6-equation two-phase model are reported in Appendix B. Next, we expand all the variables in powers of the reference Mach number  $M_{f*}$ , as for the continuous case (26). Collecting terms with equal powers of  $M_{f*}$ , one obtains at order  $M_{f*}^{-2}$  from the momentum equation (B.3):

$$\sum_{K \in v(J)} p_{m,K}^{[0]} \vec{n}_{JK} = 0. \quad (29)$$

At order  $M_{f*}^{-1}$  from the sum of the two phasic mass equations (B.2) and from the sum of the two phasic energy equations (B.4) we have

$$\sum_{K \in v(J)} \frac{1}{\hat{c}_{JK}^{[0]}} \Delta_{JK} p_m^{[0]} = 0 \quad \text{and} \quad \sum_{K \in v(J)} \frac{\hat{H}_{JK}^{[0]}}{\hat{c}_{JK}^{[0]}} \Delta_{JK} p_m^{[0]} = 0. \quad (30)$$

We notice that these discrete equations for the mixture quantities recover the form of the discrete equations of the Roe's scheme for the Euler system with the pressure  $p$  and the sound speed  $c$  of the single-phase flow replaced by  $p_m$  and by  $c_f$ , respectively. Therefore the analysis of Guillard–Viozat [12] is easily extended. First, we note that  $p_{m,K}^{[0]} = \text{constant} \forall K$  is a common solution of the equations (29), (30). We also observe that the coefficients multiplying  $\Delta_{JK} p_m^{[0]}$  in (30) are positive, hence a discrete maximum principle applies, and the extrema of the pressure field  $p_{m,K}^{[0]}$  must be on the boundary. Assuming suitable boundary conditions we can conclude that the solution  $p_{m,K}^{[0]} = \text{constant}$  is also unique. This is the case in particular if we assume that

the pressure on the boundary is a constant  $p_0$  (up to fluctuations of order  $M_{f_*}^2$ ) [12]. Now, let us consider this case  $p_{m,K}^{[0]} = \text{constant } \forall K$ , and let us use this result in the next order equations. In particular, the momentum equation (B.3) at order  $M_{f_*}^{-1}$  gives

$$\sum_{K \in \nu(J)} p_{m,K}^{[1]} \vec{n}_{JK} + \hat{\rho}_{JK}^{[0]} \hat{c}_{JK}^{[0]} \vec{n}_{JK} \Delta_{JK} U^{[0]} = 0. \quad (31)$$

In general this equation admits non-constant solutions for the order 1 pressure  $p_{m,K}^{[1]}$  [12]. Therefore we conclude that solutions of the discrete equations for the Roe-type method contain perturbations of order  $M_{f_*}$ :  $p_m(\vec{x}, t) = p_0 + p_m^{[1]}(\vec{x}, t) M_{f_*} + \dots$ , in contrast with the results for the continuous homogeneous and relaxed models, (28) and (27) respectively. The analysis for HLLC-type discretizations is analogous. Clearly, these inaccuracies remain when the mechanical relaxation step is performed by employing variables coming from the solution of the homogeneous 6-equation system. In summary, analogously to the single-phase case, there is an inconsistency in the asymptotic behavior between the continuous and discrete cases for the two-phase model, and this gives an explanation of the failure of compressible flow solvers in approximating the limit vanishing Mach number regimes [12, 13, 31].

## 6. Low Mach number preconditioning of the numerical dissipation term

As recalled in the Introduction, a classical strategy to cure the loss of accuracy of finite volume Godunov-type schemes for the Euler equations as the Mach number approaches zero consists in correcting the numerical dissipation term  $\mathcal{V} \Delta Q_{i+1/2}$ . This approach alters the order of magnitude of the entries of this term with respect to the Mach number so that the resulting discrete scheme recovers a low Mach number asymptotic behavior consistent with the one of the continuous model. Note that, since only dissipative contributions are altered, the numerical scheme remains a conservative time-consistent approximation of the system of equations [12]. Here we implement this type of low Mach number techniques to our two-phase flow model in the framework of the wave propagation algorithms described in Section 3, generalizing the approach to compressible flow model systems that are not necessarily written in fully conservative form, such the system under study here. We denote with  $\mathcal{V}^P \Delta Q_{i+1/2}$  the corrected (preconditioned) dissipation term that replaces the original one in the definition of the fluctuations in (12). As we will detail in the next subsections, for the class of preconditioning schemes considered in the present work, we can interpret the low Mach number correction as a modification of the waves and speeds of the Riemann solver that contribute to the numerical viscosity term. The preconditioned dissipation term has then the form (cf. (14)):

$$\mathcal{V}^P \Delta Q_{i+1/2} = \sum_{l=1}^{\mathcal{M}} |s_{i+1/2}^{lP}| \mathcal{W}_{i+1/2}^{lP}, \quad (32)$$

where  $s^{lP}$  and  $\mathcal{W}^{lP}$ ,  $l = 1, \dots, \mathcal{M}$ , are the preconditioned waves and speeds. Let us remark that the term  $\Delta \tilde{f}$  in (12) is still defined as in (13), by employing the original waves and speeds of the Riemann solution, and this term satisfies the property  $\Delta \tilde{f} = \Delta f$  for conservative equations.

### 6.1. A Roe-Turkel method for the six-equation two-phase flow model

We present in this Section an original extension of the Roe-Turkel method of Guillard–Viozat [12] for the Euler equations to our Roe-type scheme for the 6-equation two-phase flow model (1).

The Roe-Turkel scheme of [12] is a correction of the classical Roe's method obtained by applying Turkel's preconditioner to the Roe's dissipation term. Following this approach, the Roe's viscosity matrix for the two-phase system (Sec. 3.1.1)  $\Theta_{i+1/2} = |\hat{A}_{i+1/2}| = \hat{R}_{i+1/2} \hat{\Lambda}_{i+1/2} \hat{R}_{i+1/2}^{-1}$  is replaced by the preconditioned version

$$\Theta_{i+1/2}^P = P_{i+1/2}^{-1} |P_{i+1/2} \hat{A}_{i+1/2}|, \quad (33)$$

where  $P$  is a suitable preconditioning matrix. This matrix in the Roe-Turkel method for the Euler equations is defined as  $P^\varphi = \text{diag}(\beta^2, I_d, 1)$  on the basis of the entropic variables  $\varphi = [p, \vec{u}, s]^T$ , where  $s$  denotes the entropy and  $I_d$  denotes the identity matrix  $\in \mathbb{R}^{d \times d}$  (we recall that  $d$  indicates the spatial dimension). The parameter  $\beta \leq 1$  is of the order of the local Mach number  $M_{i+1/2}$  if  $M_{i+1/2} \leq 1$ , and equal to 1 otherwise. We now need to determine a Turkel-type preconditioning matrix for our two-phase flow model by a suitable choice of the variables of this model whose equations are going to be altered at low Mach number. The discussion in Section 5 suggests that the preconditioning factor  $\beta$ , which here is a parameter of the order of the local mixture Mach number  $M_f$ , should act on the equation for the effective pressure  $p_m = \alpha_1 p_1 + \alpha_2 p_2$ , which plays the equivalent role of the pressure  $p$  in the Euler system. Moreover, as for the Euler equations [12], we wish to correct at low Mach number only the acoustic fields of the system, and preserve unaltered interface and entropy waves corresponding to the eigenvalue  $\vec{u} \cdot \vec{n}$ . To this aim, we have chosen a Turkel-type preconditioner for our two-phase system of the form

$$P^\varphi = \text{diag}(\beta^2, I_d, 1, 1, 1, 1) \quad (34)$$

in terms of the entropic variables

$$\varphi = [p_m, \vec{u}, s_1, s_2, Y_1, \alpha_1]^T, \quad (35)$$

where  $s_k$  is the entropy of phase  $k$ . Let us remark that the volume fractions, mass fractions and phasic entropies are governed by advection equations, and these equations are preserved unaltered by the proposed preconditioner. Having defined  $P^\varphi$ , the preconditioning matrix  $P(q)$  is obtained as  $P(q) = \frac{\partial q}{\partial \varphi} P^\varphi \frac{\partial \varphi}{\partial q}$ . The transformation matrix is reported in Appendix C (for the one-dimensional case for simplicity). Finally, the preconditioned dissipation term is found as

$$\mathcal{V}^P \Delta Q_{i+1/2} = P_{i+1/2}^{-1} |P_{i+1/2} \hat{A}_{i+1/2}| (q_{i+1} - q_i) = \sum_{l=1}^7 (\hat{\zeta}_l^P |\hat{\lambda}_l^P \hat{r}_l^P)_{i+1/2}, \quad (36)$$

where  $\hat{r}_l^P = P^{-1} \hat{r}_l^P$ , and  $\hat{\lambda}_l^P, \hat{r}_l^P, l = 1, \dots, 7$ , are the eigenvalues and eigenvectors, respectively, of the matrix  $P \hat{A}$ . The coefficients  $\hat{\zeta}_l^P$  are obtained by projecting the jump  $\Delta q$  onto the basis of the eigenvectors  $\hat{r}_l^P$  as  $\Delta q = \sum_{l=1}^7 \hat{\zeta}_l^P \hat{r}_l^P$ . The expression of the preconditioned Roe eigenstructure results to be a natural extension of the one derived by Guillard–Viozat [12] for the Euler equations. As expected, only the Roe eigenstructure corresponding to the acoustic fields  $l = 1$  and  $l = 7$  is altered with respect to the original one. Below we summarize the quantities in the numerical dissipation term  $\mathcal{V} \Delta q$  that are corrected at low Mach number, namely the eigenvalues of the Roe matrix  $\hat{\lambda}_{1,7}$ , the wave strengths  $\hat{\zeta}_{1,7}$ , and the Roe eigenvectors components  $\hat{r}_{1,7}^{(\xi)}$ ,

$\xi = 4, 6, 7$ :

$$\hat{\lambda}_{1,7} = \hat{u}_{1,7} \mp \hat{c} \quad \rightarrow \quad \hat{\lambda}_{1,7}^P = \frac{1}{2}(1 + \beta^2)\hat{u} \mp \frac{1}{2}\sqrt{X_\beta} \quad (37a)$$

$$\hat{\zeta}_{1,7} = \frac{1}{2\hat{c}} \left( \frac{\Delta p_m}{\hat{c}} \mp \hat{\rho} \Delta u \right) \quad \rightarrow \quad \hat{\zeta}_{1,7}^P = \frac{1}{\sqrt{X_\beta}} \left( \frac{\Delta p_m}{\mp(\hat{\lambda}_{1,7}^P - \hat{u}\beta^2)} \mp \hat{\rho} \Delta u \right) \quad (37b)$$

$$\hat{r}_{1,7}^{(4)} = \hat{u} \mp \hat{c} \quad \rightarrow \quad \tilde{r}_{1,7}^{P(4)} = \hat{u} + (\hat{\lambda}_{1,7}^P - \hat{u}\beta^2) \quad (37c)$$

$$\hat{r}_{1,7}^{(5+k)} = \widehat{Y_k H_k} \mp \widehat{u Y_k} \hat{c} \quad \rightarrow \quad \tilde{r}_{1,7}^{P(5+k)} = \widehat{Y_k H_k} + \widehat{u Y_k} (\hat{\lambda}_{1,7}^P - \hat{u}\beta^2), \quad k = 1, 2, \quad (37d)$$

with

$$X_\beta = ((1 - \beta^2)\hat{u})^2 + (2\beta\hat{c})^2. \quad (38)$$

The fields  $l = 2, \dots, 6$  corresponding to the eigenvalue  $\hat{u}$  of the system (interface and entropy waves) remain unchanged, that is  $s^{lP} = s^l = \hat{u}$ ,  $l = 2, \dots, 6$ , and  $\sum_{l=2}^6 \mathcal{W}^{lP} = \sum_{l=2}^6 \mathcal{W}^l$ . Note in particular that the volume fraction equation is not affected by preconditioning.

When the preconditioned waves are used, we obtain a modification of the semi-discrete equations of the Roe-type scheme similar to the single-phase case [12]: terms of order  $M_{f_*}^{-2}$  appear in the phasic mass and energy equations and all terms  $M_{f_*}^{-1}$  disappear. Let us note that contributions in the equations coming from the non-conservative terms in the phasic total energy equations are at most of order 1, and they are not altered by preconditioning. By using the same asymptotic expansion approach as in Sec. 5, we obtain at order  $M_{f_*}^{-2}$  the following results from the phasic mass equations, the momentum equation and the phasic energy equations:

$$\sum_{K \in \nu(J)} \frac{\hat{Y}_{k,JK}^{[0]}}{\sqrt{\hat{X}_{\tilde{\beta},JK}^{[0]}}} \Delta_{JK} p_m^{[0]} = 0, \quad k = 1, 2, \quad (39a)$$

$$\sum_{K \in \nu(J)} p_{m,K}^{[0]} \vec{n}_{JK} + \frac{2\hat{u}_{JK}^{[0]} + \hat{U}_{JK}^{[0]} \vec{n}_{JK}}{\sqrt{\hat{X}_{\tilde{\beta},JK}^{[0]}}} \Delta_{JK} p_m^{[0]} = 0, \quad (39b)$$

$$\sum_{K \in \nu(J)} \frac{\widehat{Y_k H_k}_{JK}^{[0]}}{\sqrt{\hat{X}_{\tilde{\beta},JK}^{[0]}}} \Delta_{JK} p_m^{[0]} = 0, \quad k = 1, 2, \quad (39c)$$

where

$$\hat{X}_{\tilde{\beta},JK}^{[0]} = (\hat{U}_{JK}^{[0]})^2 + (2\tilde{\beta}\hat{c}_{JK}^{[0]})^2, \quad (39d)$$

with  $\tilde{\beta} = \frac{\beta}{M_{f_*}}$ . These equations are again analogous to the single-phase case and we can use the same arguments as for the single-phase Roe-Turkel method [12] to conclude that under suitable boundary conditions we have  $p_m(\vec{x}, t) = p_0 + p_m^{[2]}(\vec{x}, t)M_{f_*}^2 + \dots$ , as for the continuous homogeneous two-phase flow model (cf. (28)). The proof is based on the observation that  $p_m^{[0]} = \text{constant}$  is a common solution of the equations (39) above, and that the coefficients multiplying  $\Delta_{JK} p_m^{[0]}$  in (39a), (39c) are positive, hence the discrete maximum principle applies and an interior point cannot be an extremum. Moreover, since there are no terms of order  $M_{f_*}^{-1}$  in the discrete equations with preconditioned dissipation, the equations that we obtain at order  $M_{f_*}^{-1}$  when we use asymptotic expansions of the variables have the form (39) with  $p_m^{[0]}$  replaced by  $p_m^{[1]}$  [12].

Hence, we deduce perturbations for  $p_m$  of order  $M_{f*}^2$  under suitable hypotheses. This in particular holds if we assume that at the boundaries  $p_1$  and  $p_2$  are equal to a constant value  $p_0$ . We will now consider this case, and we further assume that the volume fraction at open boundaries and initially is equal to a constant value  $\alpha_{1,0}$ . Let us also note that in our fractional step algorithm Riemann data used to initialize the homogeneous two-phase system correspond to mechanical equilibrium conditions,  $p_{1,J} = p_{2,J} = p_{m,J}$ ,  $\forall J = (i, j)$ , hence the fluctuations of the phasic pressures are of the same order  $M_{f*}^2$  as those of  $p_m$ . Then, based on this, and on the fact that the volume fraction is governed by a simple advection equation independent of  $M_{f*}$  (see eq. B.1), we expect that the values of the phasic pressures and of the volume fraction coming from the the solution of the homogeneous 6-equation system are equal to constant values up to perturbations of order  $M_{f*}^2$ . When we pass to the mechanical relaxation step ( $\mu \rightarrow +\infty$ ) of the splitting algorithm the order of the fluctuations of these variables remain unchanged, since the equations used in the pressure relaxation procedure (Sec. 4) do not depend on the Mach number. We can therefore infer that the computed values of the equilibrium pressure  $p^\oplus$  and of the volume fraction  $\alpha_1^\oplus$  will also support perturbations of order  $M_{f*}^2$ ,  $M_{f*} \leq M_{W*}$ . This agrees with the results for the continuous pressure-equilibrium 5-equation model (27) discussed in Section 5 under the same hypotheses on boundary and initial conditions considered here.

As a final remark, let us note that for flows involving regimes from low subsonic ( $M_W \ll 1$ ) to supersonic ( $M_W > 1$ ) the parameter  $\beta$  should be set of the order of the mixture equilibrium Mach number  $M_W = \frac{|\bar{u}|}{c_w}$ , rather than of the order of  $M_f$ . In fact, a definition of  $\beta$  based on  $M_f$ , if  $M_f < 1 < M_W$ , might hinder the development of shocks in the simulation, and in general deteriorate the description of compressibility effects, as shown by numerical experimentation. For low Mach number flows with  $M_f \leq M_W \ll 1$  a definition of  $\beta$  based on  $M_W$  results to be a choice as effective as a definition based on  $M_f$ , based on our numerical tests.

## 6.2. An HLLC-Turkel method for the six-equation two-phase flow model

By analogy with the preconditioned wave structure of the Roe-Turkel method we propose here a low Mach number correction for our HLLC-type scheme for the two-phase flow model. The analogous preconditioning technique that we have devised for the HLLC scheme for the classical single-phase Euler equations will be detailed elsewhere. Our approach exploits the formal similarity of the acoustic wave structure of the HLLC Riemann solver with the one of the Roe's solver, which we have previously highlighted. By analogy with the Roe-Turkel method we propose the following low Mach number correction of the acoustic waves of the HLLC method. The preconditioned quantities  $S^{\ell,rP}$  and  $\check{\zeta}_{1,3}^P$  are defined as:

$$S^\ell = u_\ell - \check{c}^\ell \quad \rightarrow \quad S^{\ell P} = \frac{1}{2}(1 + \beta^2)u_\ell - \frac{1}{2}\sqrt{X_{\beta\ell}} \quad (40a)$$

$$S^r = u_r + \check{c}^r \quad \rightarrow \quad S^{rP} = \frac{1}{2}(1 + \beta^2)u_r + \frac{1}{2}\sqrt{X_{\beta r}} \quad (40b)$$

$$\check{\zeta}_1 = \frac{\rho^{*\ell}}{\rho_\ell \check{c}^\ell + \rho_r \check{c}^r} \left( \frac{\Delta p_m}{\check{c}^\ell} - \rho_r \frac{\check{c}^r}{\check{c}^\ell} \Delta u \right) \quad \rightarrow \quad \check{\zeta}_1^P = \frac{\rho^{*\ell}}{\rho_\ell \frac{\sqrt{X_{\beta\ell}}}{2} + \rho_r \frac{\sqrt{X_{\beta r}}}{2}} \left( \frac{\Delta p_m}{-(S^{\ell P} - u_\ell \beta^2)} - \rho_r \frac{\check{c}^r}{\check{c}^\ell} \Delta u \right) \quad (40c)$$

$$\check{\zeta}_3 = \frac{\rho^{*r}}{\rho_\ell \check{c}^\ell + \rho_r \check{c}^r} \left( \frac{\Delta p_m}{\check{c}^r} + \rho_\ell \frac{\check{c}^\ell}{\check{c}^r} \Delta u \right) \quad \rightarrow \quad \check{\zeta}_3^P = \frac{\rho^{*r}}{\rho_\ell \frac{\sqrt{X_{\beta\ell}}}{2} + \rho_r \frac{\sqrt{X_{\beta r}}}{2}} \left( \frac{\Delta p_m}{S^{rP} - u_r \beta^2} + \rho_\ell \frac{\check{c}^\ell}{\check{c}^r} \Delta u \right) \quad (40d)$$

where

$$X_{\beta\ell} = ((1 - \beta^2)u_\ell)^2 + (2\beta\check{c}^\ell)^2 \quad \text{and} \quad X_{\beta r} = ((1 - \beta^2)u_r)^2 + (2\beta\check{c}^r)^2. \quad (40e)$$

For the vectors  $\check{r}_{1,3}$  we alter the following components:

$$\check{r}_1^{(4)} = u_\ell - \check{c}^\ell \quad \rightarrow \quad \check{r}_1^{P(4)} = u_\ell + (S^{\ell P} - u_\ell \beta^2) \quad (40f)$$

$$\check{r}_1^{(5+k)} = Y_{k,\ell}(H_{k,\ell} - S^\star \check{c}^\ell) \quad \rightarrow \quad \check{r}_1^{P(5+k)} = Y_{k,\ell}(H_{k,\ell} + S^\star(S^{\ell P} - u_\ell \beta^2)), \quad k = 1, 2, \quad (40g)$$

$$\check{r}_3^{(4)} = u_r + \check{c}^r \quad \rightarrow \quad \check{r}_3^{P(4)} = u_r + (S^{rP} - u_r \beta^2) \quad (40h)$$

$$\check{r}_3^{(5+k)} = Y_{k,r}(H_{k,r} + S^\star \check{c}^r) \quad \rightarrow \quad \check{r}_3^{P(5+k)} = Y_{k,r}(H_{k,r} + S^\star(S^{rP} - u_r \beta^2)), \quad k = 1, 2. \quad (40i)$$

As for the Roe-Turkel method, we maintain unaltered the contact wave:  $s^{2P} = S^\star$ ,  $\mathcal{W}^{2P} = \mathcal{W}^2$ . The parameter  $\beta$  is defined as indicated in the previous section by using a local Mach number that can be computed for instance as  $M_{i+1/2} = M_{\ell r} = \min\left(\frac{|\vec{u}_\ell|}{\check{c}^\ell}, \frac{|\vec{u}_r|}{\check{c}^r}\right)$ . The preconditioned waves are used to compute the dissipation term (32) of the scheme. This correction of the HLLC method produces a rescaling of contributions to the numerical dissipation term with respect to the Mach number that is analogous to the one of the Roe-Turkel method. Let us finally remark that our Turkel-type preconditioning strategy for the HLLC-type scheme differs from the preconditioned HLLC-type method employed in [30] for the internal-energy-based formulation of the 6-equation two-phase model [2]. The authors in [30] follow to some extent the approach of the preconditioned Riemann problem of [13, 28]. More specifically, the method in [30] uses the same correction of the wave speeds  $S^\ell$ ,  $S^r$  as in (40a), (40b) (with  $\hat{c}^{\ell,r} = c_{\ell,r}$ ), however, in contrast to our technique, these modified speeds are used to replace the original ones in the other formulas of the standard HLLC Riemann solver (e.g. speed  $S^\star$ ), together with a separate treatment of the equations for the phasic specific internal energies, which are approximated by advection equations at low Mach number.

## 7. Numerical experiments

We present in this Section some numerical experiments aimed at showing the effectiveness of the proposed preconditioning techniques in curing the problem of loss of accuracy at low Mach number regimes of the standard Roe-type and HLLC-type schemes [1] for the six-equation two-phase flow model (1). Since the objective is to study the effect of preconditioning of the numerical dissipation tensor, and to verify numerically some theoretical results inferred by the analysis of first-order schemes, we present results that are first-order accurate, avoiding the interference of effects of higher order terms.

### 7.1. Low Mach number two-phase channel flow

We first perform a two-phase liquid-gas channel flow numerical experiment analogous to a single-phase channel flow test presented in [18]. Similar two-phase nozzle flow tests were also solved in [28] for the 5-equation model (4) and in [40] for a simpler homogeneous mixture model. We simulate a two-dimensional flow ( $\vec{u} = (u, v)$ ,  $\vec{x} = (x, y)$ ) in a channel of length = 4 m and height = 1 m with a bump defined by  $y = (1 - \cos((x - 1)\pi))/10$ , if  $x \in [1, 3]$ , and  $y = 0$  otherwise. We consider a flow of liquid water initially containing a uniformly distributed small amount of gas,  $\alpha_{g0} = 10^{-3}$ . The EOS parameters for the two phases are  $\gamma_l = 2.35$ ,  $\varpi_l = 10^9$  Pa,  $\eta_l = -1167 \times 10^3$  J/kg,  $\gamma_g = 1.43$ ,  $\varpi_g = 0$  Pa,  $\eta_g = 2030 \times 10^3$  J/kg. We set an inlet pressure  $p_0 = 10^6$  Pa and an inlet temperature for both phases  $T_0 = 458.63$  K. The corresponding values of the phase densities are found as  $\rho_{l0} = 890.27$  kg/m<sup>3</sup> and  $\rho_{g0} = 4.88$  kg/m<sup>3</sup>, for liquid and gas, respectively (with heat capacities at constant volume  $C_{vl} = 1816$  J/(kg K),

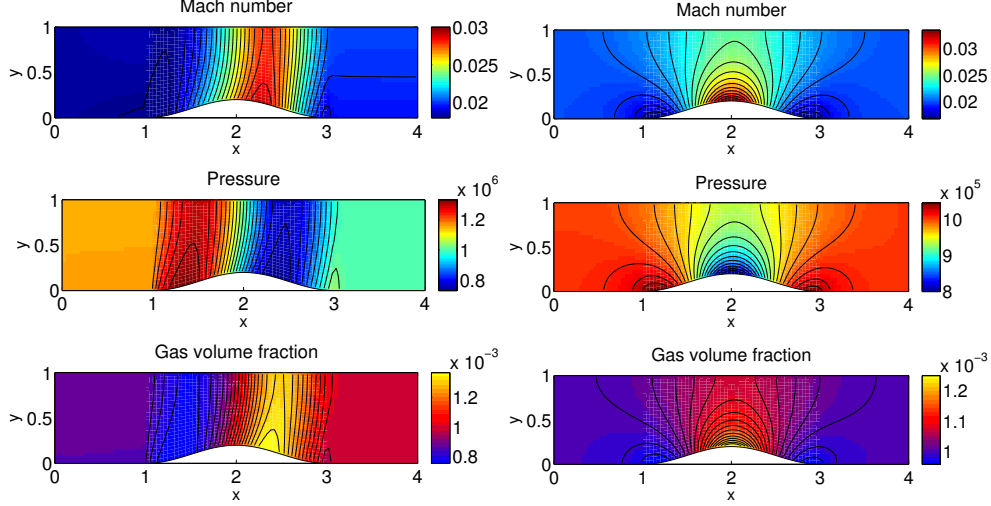


Figure 2: Numerical results for the two-phase liquid-gas channel flow test with  $M_0 = 0.01999$  ( $u_0 = 20$  m/s) obtained with the Roe's scheme (left column) and the Roe-Turkel scheme (right column) at stationary conditions. From top to bottom: Mach number, pressure, and gas volume fraction.

$C_{vg} = 1040 \text{ J}/(\text{kg K})$ ). We impose an inlet velocity  $\vec{u}_0 = (u_0, 0)$  and an outlet pressure  $p_0$ . The velocity downstream is extrapolated from the interior domain. The values  $u_0, p_0, \rho_{l0}, \rho_{g0}$  are also used for the initial conditions. Boundary conditions are implemented following the method detailed in [54]. The preconditioning parameter  $\beta$  is defined locally for each Riemann problem as  $\beta = \min(\max(\epsilon, M_{tr}), 1)$ , with  $\epsilon = 10^{-10}$  (a tolerance used to avoid the singularity of the preconditioned quantities that may occur for  $|\vec{u}| = 0$ ). The average local Mach number  $M_{tr}$  used for the results presented for this low Mach number tests is based on the frozen Mach number  $M_f$ . Nonetheless, we have also run some of the experiments reported here with a definition of  $\beta$  based on the equilibrium Mach number  $M_W$ , and no relevant differences were observed. We perform simulations for four different decreasing values of the inlet velocity:  $u_0 = 20, 10, 5, 2$  m/s. With this setup the reference inlet Mach number  $M_* = M_0$  of the equilibrium mixture for the four cases is  $M_0 = \frac{u_0}{c_{w0}} = 0.01999, 0.00999, 0.00499, 0.00199$  (hence it ranges roughly from  $2 \times 10^{-2}$  to  $2 \times 10^{-3}$ ). The reference equilibrium sound speed (Wood's sound speed) is  $c_{w0} = 1.00017 \times 10^3$  m/s. Note that the frozen sound speed is  $c_{f0} = 1.62551 \times 10^3$  m/s  $> c_{w0}$ . The considered range of the Mach number for these numerical tests is relevant for some application problems of interest, such as the simulation of cavitating flows in Venturi tubes [55, 30] or around hydrofoils [56]. The two-phase flow in this problem is expected to reach a subsonic stationary regime with a slight pressure drop and a small gas volume fraction increase in correspondence of the channel restriction, as we can infer from the exact quasi-one-dimensional steady solution that can be derived for liquid-gas nozzle flows [57]. Simulations are performed with the standard Roe-type scheme (in the sequel named sometimes Roe's scheme for simplicity) and the preconditioned Roe-type and HLLC-type schemes on a computational grid with  $100 \times 25$  cells. We stop the simulations at a time at which stationary conditions can be considered attained. The criterion used to establish if steady conditions have been approximately reached is based on a tolerance  $\epsilon_s = 10^{-4}$  on the relative variation in time

of pressure and mixture density maximum fluctuations,  $\delta p_{\max} = \frac{p_{\max} - p_{\min}}{p_0}$  and  $\delta \rho_{\max} = \frac{\rho_{\max} - \rho_{\min}}{\rho_0}$ , respectively.

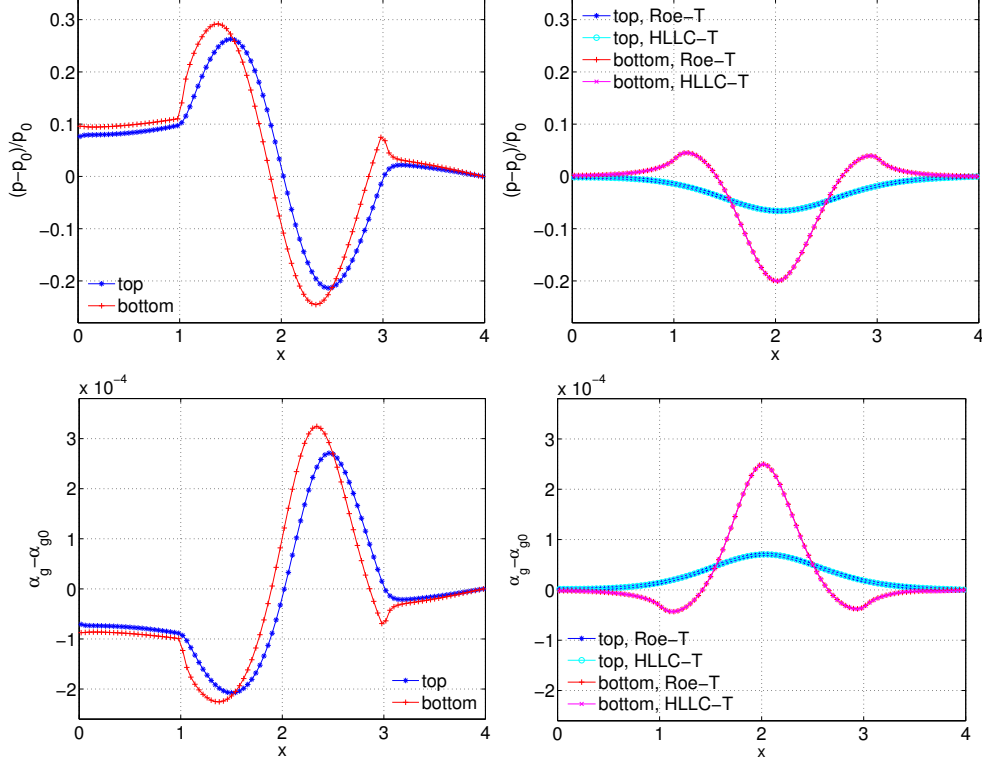


Figure 3: Numerical results for the two-phase liquid-gas channel flow test with  $M_0 = 0.01999$  ( $u_0 = 20$  m/s). Profiles of the normalized pressure fluctuations (upper plots) and of the volume fraction fluctuations (lower plots) at the top and at the bottom of the channel (see also Fig. 2). Left: results obtained by the Roe's scheme; Right: results obtained by the Roe-Turkel and HLLC-Turkel schemes (results are superimposed).

We begin by showing in Figure 2 a comparison of the results obtained with the Roe's scheme (left column) and with the Roe-Turkel scheme (right column) for the case with higher Mach number  $M_0 = 0.01999$  ( $u_0 = 20$  m/s). Here we display from top to bottom pseudo-color plots of the Mach number of the equilibrium mixture  $M = \frac{|u|}{c_w}$ , the mixture pressure  $p$ , and the gas volume fraction  $\alpha_g$ . Moreover, in Figure 3 we show the profiles of the normalized pressure fluctuations  $\frac{p-p_0}{p_0}$  and of the volume fraction fluctuations  $\alpha_g - \alpha_{g0}$  along the upper and lower boundaries of the channel for the computations with the Roe's scheme (left) and the Roe-Turkel and HLLC-Turkel schemes (right). With all the schemes the flow reaches a steady subsonic configuration. The correct solution behavior is captured however only when Turkel's preconditioning is activated. In contrast with the results of the Roe-Turkel and HLLC-Turkel methods, the solution computed by the standard Roe-type scheme is non-symmetric and deviates from the correct one. In Figures 4, 5 and 6 we show results obtained for the test case with the lower inlet Mach number  $M_0 = 0.0019$  ( $u_0 = 2$  m/s). In Figure 4 we display pseudo-color plots of the Mach number, pressure and volume fraction obtained with the Roe-Turkel scheme, and the pseudo-color plot of the Mach

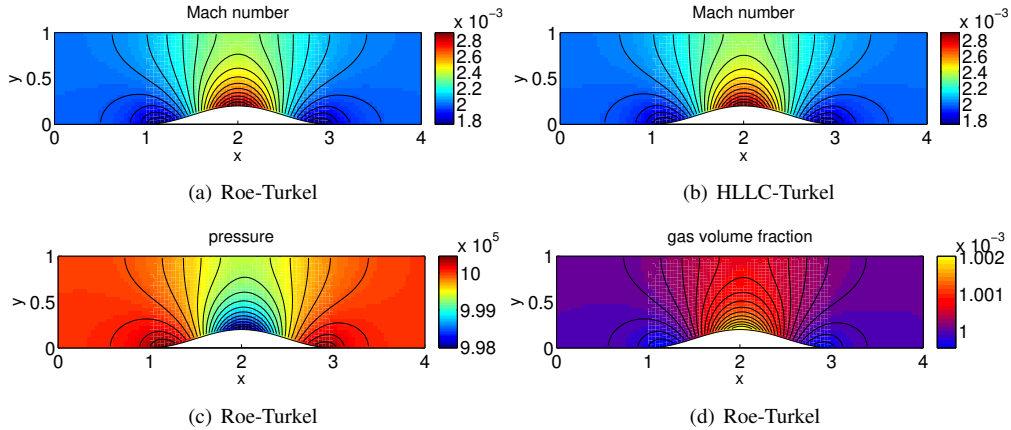


Figure 4: Numerical results for the two-phase liquid-gas channel flow test with  $M_0 = 0.00199$  ( $u_0 = 2$  m/s). (a), (c), (d): Mach number, pressure, and gas volume fraction, respectively, computed by the Roe-Turkel scheme. (b): Mach number computed by the HLLC-Turkel scheme.

number obtained with the HLLC-Turkel scheme. We omit plots of other variables for the HLLC-Turkel scheme since results of the two schemes do not present relevant differences. This is indeed not surprising considering the similar wave structure of the two solvers and the small perturbations that characterize the solution of these tests. In Figure 5 we compare the profiles at the upper and lower boundaries of the Mach number, normalized pressure, gas volume fraction and horizontal velocity computed by the preconditioned Roe's and HLLC schemes. In the same plots we also show the profiles of the average quantities over the channel height computed by the Roe-Turkel scheme together with the exact steady quasi-one-dimensional two-phase channel flow solution that can be obtained for the five-equation pressure equilibrium model for the chosen set of initial and boundary conditions [57]. We see that also for this lower value  $M_0 = 0.0019$  of the inlet Mach number the preconditioned methods are able to capture accurately the correct features of the flow field. A reasonable qualitative agreement of the solution behavior is observed between the 2D computed solution and the exact steady quasi-1D solution. In Figure 6 we display the pressure fluctuations  $\frac{p_b - p_0}{p_0}$  and the volume fraction fluctuations  $\alpha_{gb} - \alpha_{g0}$  along the bottom boundary at different times, from  $t = 0.002$  s to  $t = 0.062$  s, time at which stationary conditions are approximately reached (plots in Figures 4 and 5 correspond to  $t = 0.08$  s). We can observe the monotonic decrease of fluctuations in the transition period towards the stationary state, indicating the stability of the preconditioning approach.

Following the idea of [12], to assess the accuracy of the Roe-Turkel and HLLC-Turkel methods at low Mach number we have also computed the maximum pressure and volume fraction fluctuations in the whole flow domain  $\delta p_{\max} = \frac{p_{\max} - p_{\min}}{p_0}$  and  $\delta \alpha_{g \max} = \alpha_{g \max} - \alpha_{g \min}$ , respectively, for decreasing reference (inlet) Mach number  $M_0$  for the set of considered experiments. The results are reported in Table 1 for the Roe's scheme and the Roe-Turkel scheme. The results for the HLLC-Turkel scheme are of the same order of those of the Roe-Turkel scheme, and equal to those of the Roe-Turkel scheme at least for the first three significant digits. Moreover, we display in Figure 7 a log-log plot of the values of  $\delta p_{\max}$  (left) and  $\delta \alpha_{g \max}$  (right) versus  $M_0$  for the Roe's scheme, the Roe-Turkel scheme and the HLLC-Turkel scheme. We can observe that for the Roe-Turkel scheme and for the HLLC-Turkel scheme perturbations correctly scale with the square of

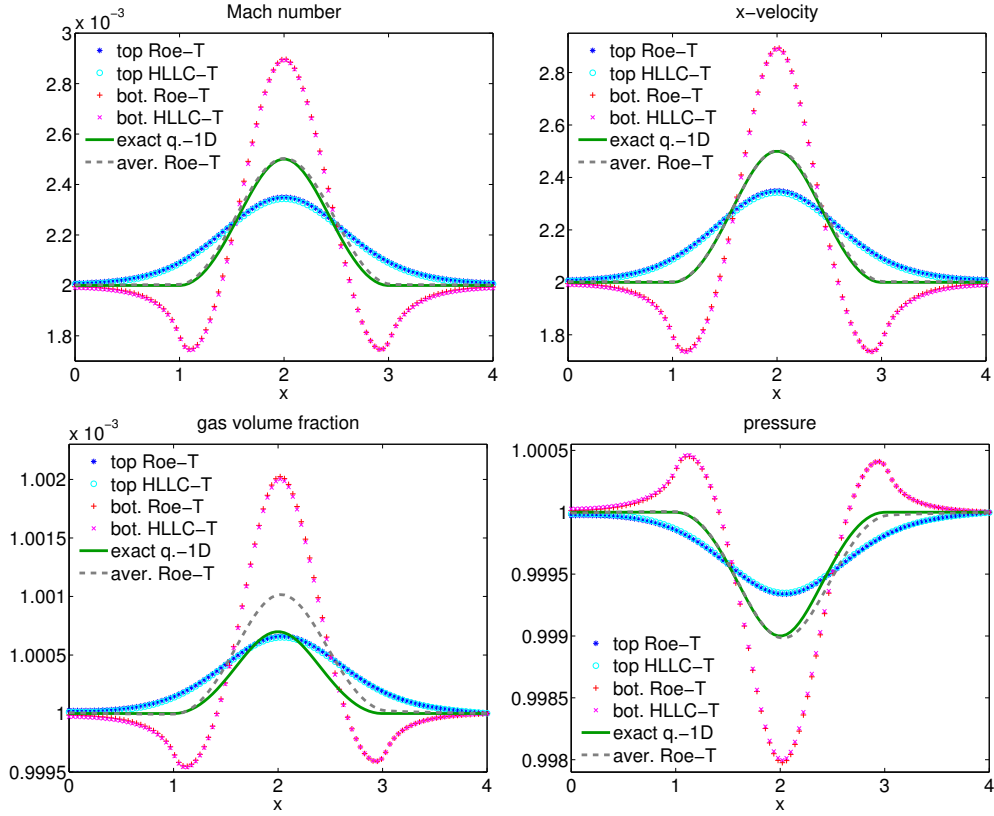


Figure 5: Results for the two-phase liquid-gas channel flow test with  $M_0 = 0.00199$  ( $u_0 = 2$  m/s). Profiles at the top and bottom boundaries of the Mach number, horizontal velocity, gas volume fraction and normalized pressure  $p/p_0$  computed by the Roe-Turkel and HLLC-Turkel schemes, average quantities over the channel height given by the Roe-Turkel scheme, and exact quasi-one-dimensional steady state solution.

the Mach number  $M_0$  consistently with the theoretical results, at least for the considered range of the Mach number. The Roe's scheme produces perturbations that have approximately a linear variation with  $M_0$ .

$u_0$ [m/s]	$M_0$	$\delta p_{\max}$ (R-T)	$\delta p_{\max}$ (Roe)	$\delta \alpha_{g \max}$ (R-T)	$\delta \alpha_{g \max}$ (Roe)
20	0.01999	0.24553	0.59704	$2.9309 \times 10^{-4}$	$6.1179 \times 10^{-4}$
10	0.00999	0.06135	0.27800	$6.3731 \times 10^{-5}$	$2.6857 \times 10^{-4}$
5	0.00499	0.01535	0.13519	$1.5473 \times 10^{-5}$	$1.3122 \times 10^{-4}$
2	0.00199	0.00247	0.05373	$2.4742 \times 10^{-6}$	$5.2907 \times 10^{-5}$

Table 1: Values of the pressure fluctuations  $\delta p_{\max} = \frac{p_{\max} - p_{\min}}{p_0}$  and of the volume fraction fluctuations  $\delta \alpha_{g \max} = \alpha_{g \max} - \alpha_{g \min}$  computed by the Roe-Turkel method (R-T) and by the Roe's method for the liquid-gas channel flow experiment for decreasing values of the inlet Mach number  $M_0$ .

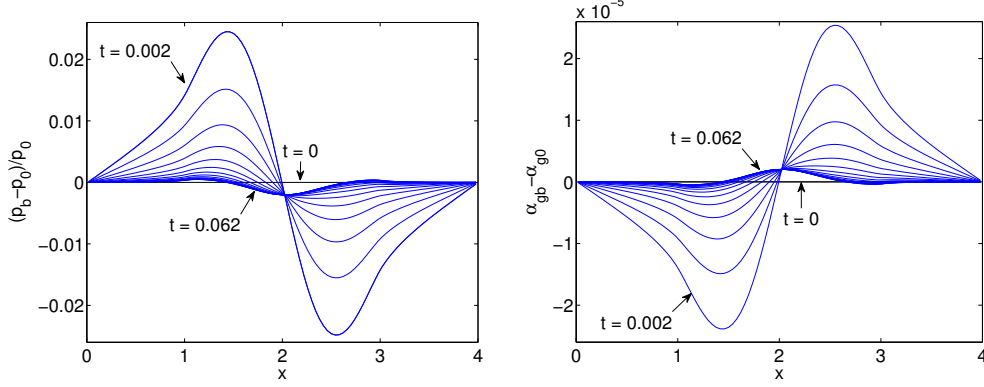


Figure 6: Results for the two-phase liquid-gas channel flow test with  $M_0 = 0.00199$  ( $u_0 = 2$  m/s). Profiles of the bottom pressure fluctuations (left) and of the bottom volume fraction fluctuations (right) from time  $t = 0.002$  s to  $t = 0.062$  s with intervals of 4 ms.

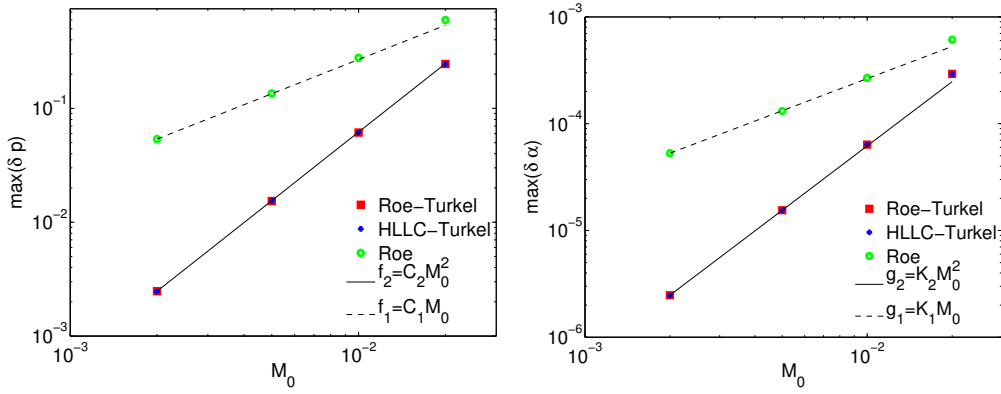


Figure 7: Log-log plot of the pressure fluctuations  $\delta p_{\max}$  and of the volume fraction fluctuations  $\delta \alpha_{g \max}$  versus the inlet Mach number  $M_0$  computed by the Roe-Turkel scheme, the HLLC-Turkel scheme, and by the Roe's scheme for the channel flow tests performed (see also Table 1). The reference curves  $f_j(M_0) = C_j M_0^j$  and  $g_j(M_0) = K_j M_0^j$ ,  $j = 1, 2$ , which are straight lines of slope  $j$  in the log-log graphs, are also drawn in the plots for the pressure and volume fraction fluctuations, respectively, to observe more easily the behavior of the fluctuations with respect to  $M_0^j$ . The constant factors  $C_j, K_j$  are determined so that  $f_j$  and  $g_j$  pass through the point corresponding to results obtained with the Roe-Turkel method ( $j = 2$ ) and the Roe's method ( $j = 1$ ) for the test case with the lowest inlet Mach number  $M_0 = 0.00199$ .

## 7.2. Two-phase transonic nozzle flow

We perform now a numerical experiment with the preconditioned schemes for a two-phase transonic channel flow. The purpose is to observe the capability of the preconditioned methods to describe Mach number regimes from low subsonic to supersonic with strong compressibility effects and shock formation. The channel geometry is analogous to the one used in the previous subsonic channel flow tests, but we change the channel height, which here is set to 0.48 m, and the channel length, which is set to 3.62 m. The setup of the problem is also similar to the previous experiments: we consider again a liquid flow with an initial small amount of gas,  $\alpha_{g0} = 10^{-3}$ . The inlet and initial densities are  $\rho_{l0} = 1.15 \times 10^{-3}$  kg/m<sup>3</sup> and  $\rho_{g0} = 1$  kg/m<sup>3</sup> for liquid and

gas, respectively. The inlet and initial pressure is  $p_{\text{in}} = 1.3 \times 10^7$  Pa, and the outlet pressure is  $p_{\text{out}} = 0.9 \times 10^7$  Pa. The inlet velocity is 100 m/s, hence the inlet (equilibrium) Mach number is  $M_{\text{in}} = 0.0737$ . We use a grid with  $201 \times 25$  cells. As mentioned previously, for this test a definition of  $\beta$  based on  $M_{\text{W}}$  is necessary in order to model shock waves. Numerical results obtained by the Roe-Turkel and HLLC-Turkel schemes are similar, and here we report in Figure 8 pseudo-color plots of the Mach number, gas volume fraction and pressure obtained with the Roe-Turkel method. In the same figure, on the right, we show the profiles of the pressure at the top and bottom boundaries computed by the two preconditioned schemes. In this channel flow problem the flow is subsonic in the converging section of the channel, where it accelerates reaching sonic conditions at the throat. In the diverging section of the channel the flow is first supersonic and then it becomes subsonic through a shock, clearly visible from the discontinuities in the flow variables in Figure 8. We can observe the growth of a significant gas cavity in correspondence of the supersonic flow region with low pressure. The Mach number ranges from a minimum value of 0.017 to a maximum value of 26.555. This large variation of the Mach number is related to the non-monotonic behaviour of Wood's sound speed with respect to the volume fraction, see Figure 1. In particular, the speed of sound of the equilibrium mixture can reach very small values, compared to the speed of sound of the nearly pure phases. For this reason we observe in Figure 8 that the highest values of the Mach number are attained in correspondence of the region of the mixture with values of the gas volume fraction around 0.5.

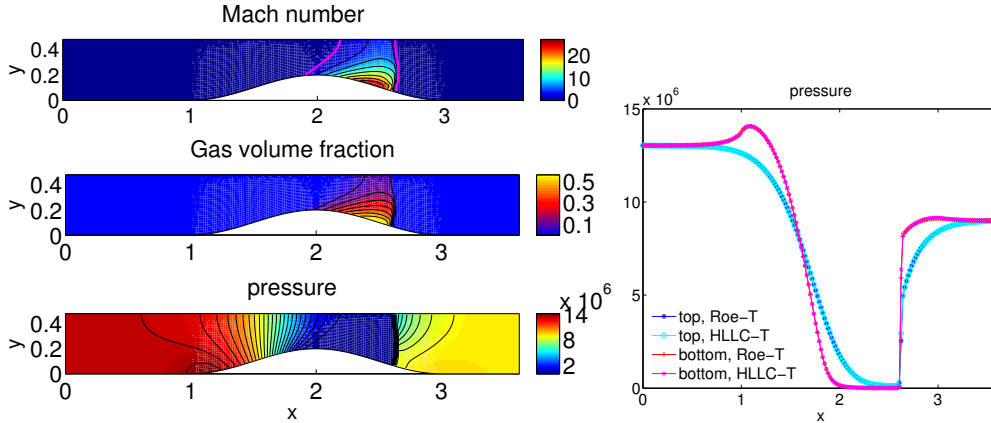


Figure 8: Transonic liquid-gas flow in a channel with a restriction with normal shock formation in the divergent section,  $u_0 = 100$  m/s,  $M_0 = 0.073750$ . Left: pseudo-color plots of the Mach number, gas volume fraction, pressure computed by the Roe-Turkel scheme. The two thick pink lines in the plot of the Mach number indicate the sonic lines  $M = 1$ . Right: profiles of the pressure on the top and bottom boundaries computed by the Roe-Turkel and HLLC-Turkel schemes.

## 8. Conclusions

In this paper we have developed original low Mach number preconditioning techniques for the wave propagation schemes that we have presented in previous work [1] for a two-phase compressible flow model with stiff pressure relaxation. Extending the method of Guillard-Viozat [12] for the single-phase Euler equations, we have first derived a Turkel-type [9] preconditioner for our Roe-type method for the two-phase system. The analysis via asymptotic

expansions of the preconditioned Roe's discrete two-phase equations shows that preconditioning acts as in the single-phase case, namely the low Mach number correction allows one to recover the correct scaling of pressure perturbations. We have then devised analogous corrections of the numerical dissipation term at low Mach number for the HLLC-type method for our two-phase flow model. This was possible thanks to a reformulation of the HLLC Riemann solver, which highlights the formal similarity of the acoustic wave structure of the HLLC Riemann solver with the one of the Roe solver. Although for the problems presented here the Roe-Turkel and the HLLC-Turkel methods exhibit analogous performance, based on our previous experience [1] the HLLC-Turkel method is expected to be more robust for computations with the full six-equation two-phase flow model with heat and mass transfer terms, which is ultimately the model that we wish to employ to describe phase transition processes. The preconditioned methods that we have studied have been formulated in the framework of wave propagation schemes, which use quantities expressed in terms of the numerical wave structure at interfaces rather than numerical fluxes. This in particular establishes a convenient framework to apply preconditioning to schemes for hyperbolic systems that are not in fully conservative form. Numerical experiments for low Mach number problems show the effectiveness of the preconditioned methods for the two-phase flow model. In particular the results indicate that the order of pressure fluctuations supported at the discrete level at low Mach number agrees with the theoretical results for the relaxed continuous pressure equilibrium model, obtained via an asymptotic analysis by Murrone–Guillard [28].

This paper has focused on the problem of loss of accuracy at low Mach number regimes related to the spatial discretization of convective terms, and preconditioning techniques as a remedy to this difficulty. However, for practical applications, it is essential to address the issue of the extremely severe time step restriction demanded for stability at low Mach number by explicit time integrations, cf. [36]. For this, we plan to develop implicit time integration techniques, following for instance [38, 30, 58].

**Acknowledgments.** The present work was supported by DGA, the French Government Directorate for Armament (*Direction Générale de l'Armement*), in the framework of a research project funded by DGA on “Full-Mach-number-range numerical simulation of cavitating flows by multiphase compressible flow models”, Grants DGA N. 2009.60.035.00.470.75.01 and DGA N. 2012.60.0011.00.470.75.01. The author has been also partially supported by the Research Council of Norway in the framework of the SIMCOFLOW Project, Grant RCN N. 234126/E30.

## Appendix A. Roe eigenstructure for the six-equation two-phase flow model

We write here the expression of the eigenstructure of the Roe matrix  $\hat{A}(q_\ell, q_r)$  for a plane-wave Riemann problem with data  $q_\ell, q_r$  in the  $x$  direction for the two-dimensional six-equation two-phase flow model. We begin by defining the following averaged quantities:

$$\hat{u} = \frac{u_\ell \sqrt{\rho_\ell} + u_r \sqrt{\rho_r}}{\sqrt{\rho_\ell} + \sqrt{\rho_r}}, \quad \hat{v} = \frac{v_\ell \sqrt{\rho_\ell} + v_r \sqrt{\rho_r}}{\sqrt{\rho_\ell} + \sqrt{\rho_r}}, \quad \hat{\rho} = \sqrt{\rho_\ell \rho_r}, \quad (\text{A.1a})$$

$$\hat{Y}_k = \frac{Y_{k\ell} \sqrt{\rho_\ell} + Y_{kr} \sqrt{\rho_r}}{\sqrt{\rho_\ell} + \sqrt{\rho_r}}, \quad \widehat{Y_k H_k} = \frac{(Y_k H_k)_\ell \sqrt{\rho_\ell} + (Y_k H_k)_r \sqrt{\rho_r}}{\sqrt{\rho_\ell} + \sqrt{\rho_r}}, \quad (\text{A.1b})$$

$$\widehat{u Y_k} = \frac{(u Y_k)_\ell \sqrt{\rho_\ell} + (u Y_k)_r \sqrt{\rho_r}}{\sqrt{\rho_\ell} + \sqrt{\rho_r}}, \quad \widehat{v Y_k} = \frac{(v Y_k)_\ell \sqrt{\rho_\ell} + (v Y_k)_r \sqrt{\rho_r}}{\sqrt{\rho_\ell} + \sqrt{\rho_r}}, \quad (\text{A.1c})$$

$$\widehat{u Y_k} = \frac{1}{2} (\hat{u} \hat{Y}_k + \widehat{u Y_k}), \quad \widehat{v Y_k} = \frac{1}{2} (\hat{v} \hat{Y}_k + \widehat{v Y_k}), \quad k = 1, 2, \quad \hat{\mathcal{K}} = \frac{\hat{u}^2 + \hat{v}^2}{2}, \quad (\text{A.1d})$$

$$\hat{c} = \sqrt{\widehat{Y_1 c_1^2} + \widehat{Y_2 c_2^2}}, \quad \widehat{Y_k c_k^2} = \kappa_k (\widehat{Y_k H_k} - \hat{\mathcal{K}} \hat{Y}_k) + \chi_k \hat{Y}_k, \quad k = 1, 2. \quad (\text{A.1e})$$

The Roe eigenvalues are found as

$$\hat{\lambda}_1 = \hat{u} - \hat{c}, \quad \hat{\lambda}_2 = \hat{\lambda}_3 = \hat{\lambda}_4 = \hat{\lambda}_5 = \hat{\lambda}_6 = \hat{u}, \quad \hat{\lambda}_7 = \hat{u} + \hat{c}, \quad (\text{A.2})$$

and the corresponding matrix of the Roe right eigenvectors is

$$\hat{R} = \begin{pmatrix} 0 & 0 & 0 & 0 & 1 & 0 & 0 \\ \hat{Y}_1 & 0 & 0 & 1 & 0 & 0 & \hat{Y}_1 \\ \hat{Y}_2 & 0 & 1 & 0 & 0 & 0 & \hat{Y}_2 \\ \hat{u} - \hat{c} & 0 & \hat{u} & \hat{u} & 0 & 0 & \hat{u} + \hat{c} \\ \hat{v} & 0 & 0 & 0 & 0 & 1 & \hat{v} \\ \widehat{Y_1 H_1} - \widehat{u Y_1} \hat{c} & -\frac{\kappa_2}{\kappa_1} & -\frac{\chi_2}{\kappa_1} + \frac{\kappa_2}{\kappa_1} \hat{\mathcal{K}} - \hat{v} \frac{\hat{V}}{\kappa_1} & -\frac{\chi_1}{\kappa_1} + \hat{\mathcal{K}} - \hat{v} \frac{\hat{V}}{\kappa_1} & \frac{\gamma_1 \varpi_1 - \gamma_2 \varpi_2}{\kappa_1} & \frac{\hat{V}}{\kappa_1} & \widehat{Y_1 H_1} + \widehat{u Y_1} \hat{c} \\ \widehat{Y_2 H_2} - \widehat{u Y_2} \hat{c} & 1 & 0 & 0 & 0 & 0 & \widehat{Y_2 H_2} + \widehat{u Y_2} \hat{c} \end{pmatrix}, \quad (\text{A.3})$$

where  $\hat{V} = \kappa_1 \widehat{v Y_1} + \kappa_2 \widehat{v Y_2}$ , and  $\kappa_k = (\gamma_k - 1)$ ,  $\chi_k = -(\gamma_k - 1)\eta_k$ ,  $k = 1, 2$ . The coefficients  $\hat{\zeta}_l$ ,  $l = 1, \dots, 7$ , of the Roe eigen-decomposition  $q_r - q_\ell = \sum_{l=1}^7 \hat{\zeta}_l \hat{r}_l$ , are given by

$$\hat{\zeta}_1 = \frac{1}{2\hat{c}} \left( \frac{\Delta p_m}{\hat{c}} - \hat{\rho} \Delta u \right), \quad \hat{\zeta}_7 = \frac{1}{2\hat{c}} \left( \frac{\Delta p_m}{\hat{c}} + \hat{\rho} \Delta u \right), \quad \hat{\zeta}_5 = \Delta \alpha_1, \quad (\text{A.4a})$$

$$\hat{\zeta}_2 = \Delta(\alpha_2 E_2) - \frac{\Delta p_m}{\hat{c}^2} \widehat{Y_2 H_2} - \hat{\rho} \widehat{u Y_2} \Delta u = -\frac{\Delta p_m}{\hat{c}^2} \widehat{Y_2 H_2} + \hat{\mathcal{K}} \Delta(\alpha_2 \rho_2) + \Delta(\alpha_2 \mathcal{E}_2) + \hat{\rho} \widehat{v Y_2} \Delta v, \quad (\text{A.4b})$$

$$\hat{\zeta}_3 = \Delta(\alpha_2 \rho_2) - \hat{Y}_2 \frac{\Delta p_m}{\hat{c}^2}, \quad \hat{\zeta}_4 = \Delta(\alpha_1 \rho_1) - \hat{Y}_1 \frac{\Delta p_m}{\hat{c}^2}, \quad \hat{\zeta}_6 = \hat{\rho} \Delta v + \hat{v} \left( \Delta \rho - \frac{\Delta p_m}{\hat{c}^2} \right), \quad (\text{A.4c})$$

where  $\Delta(\cdot) \equiv (\cdot)_r - (\cdot)_\ell$  and where we recall that  $p_m = \alpha_1 p_1 + \alpha_2 p_2$ . Let us remark that although we have chosen to write the eigenvectors  $\hat{r}_l$  associated to the eigenvalue  $\hat{\lambda}_l = \hat{u}$ ,  $l = 2, \dots, 6$ , in a form that is not symmetric with respect to the components corresponding to the phasic total energy equations, we have, as expected, symmetric expressions for the total jump across the interface wave moving at speed  $\hat{u}$ , that is  $\sum_{l=2}^6 \mathcal{W}^{l(k+5)} = \sum_{l=2}^6 \hat{\zeta}_l \hat{r}_l^{(k+5)} = \Delta(\alpha_k E_k) - \frac{\Delta p_m}{\hat{c}^2} \widehat{Y_k H_k} - \hat{\rho} \widehat{u Y_k} \Delta u = -\frac{\Delta p_m}{\hat{c}^2} \widehat{Y_k H_k} + \hat{\mathcal{K}} \Delta(\alpha_k \rho_k) + \Delta(\alpha_k \mathcal{E}_k) + \hat{\rho} \widehat{v Y_k} \Delta v$ ,  $k = 1, 2$ .

## Appendix B. Semi-discrete equations of the Roe-type scheme for the two-phase system

The non-dimensionalized two-dimensional semi-discrete equations of the first order Roe-type scheme for the 6-equation two-phase model are obtained from (6) by using the Roe wave structure reported in Appendix A. We use here the grid notation introduced in Section 5, and we set  $M_* = M_{f_*}$  for simplicity.

*Volume fraction equation*

$$\delta \frac{d\alpha_{1,J}}{dt} + \frac{1}{2} \sum_{K \in \nu(J)} (|\hat{U}_{JK}| - \hat{U}_{JK}) \Delta_{JK} \alpha_1 = 0. \quad (\text{B.1})$$

*Mass equations*

$$\delta \frac{d(\alpha_k \rho_k)_J}{dt} + \frac{1}{2} \sum_{K \in \nu(J)} (\alpha_k \rho_k)_K \vec{u}_K \cdot \vec{n}_{JK} + \frac{1}{2} \sum_{K \in \nu(J)} |\hat{U}_{JK}| \left( \Delta_{JK} (\alpha_k \rho_k) - \hat{Y}_{k,JK} \frac{\Delta_{JK} p_m}{\hat{c}_{JK}^2} \right) \quad (\text{B.2a})$$

$$+ \frac{1}{2M_*} \sum_{K \in \nu(J)} \hat{Y}_{k,JK} \frac{\Delta_{JK} p_m}{\hat{c}_{JK}} + \frac{M_*}{2} \sum_{K \in \nu(J)} \hat{Y}_{k,JK} \frac{\hat{\rho}_{JK} \hat{U}_{JK}}{\hat{c}_{JK}} \Delta_{JK} U = 0, \quad k = 1, 2. \quad (\text{B.2b})$$

The contributions to the numerical dissipation term associated to the contact wave appear in the last term of (B.2a), while contributions associated to the acoustic waves are those in (B.2b).

*Momentum equation*

$$\delta \frac{d(\rho \vec{u})_J}{dt} + \frac{1}{2} \sum_{K \in \nu(J)} (\rho \vec{u})_K (\vec{u}_K \cdot \vec{n}_{JK}) + \frac{1}{2M_*^2} \sum_{K \in \nu(J)} p_{m,K} \vec{n}_{JK} \quad (\text{B.3a})$$

$$+ \frac{1}{2} \sum_{K \in \nu(J)} |\hat{U}_{JK}| \left( \left( \Delta_{JK} \rho - \frac{\Delta_{JK} p_m}{\hat{c}_{JK}^2} \right) \vec{u}_{JK} + \hat{\rho}_{JK} \vec{n}_{JK}^\perp \Delta_{JK} V \right) \quad (\text{B.3b})$$

$$+ \frac{1}{2M_*} \sum_{K \in \nu(J)} (\hat{U}_{JK} \vec{n}_{JK} + \vec{u}_{JK}) \frac{\Delta_{JK} p_m}{\hat{c}_{JK}} + \hat{\rho}_{JK} \hat{c}_{JK} \vec{n}_{JK} \Delta_{JK} U + \frac{M_*}{2} \sum_{K \in \nu(J)} \frac{\hat{\rho}_{JK} \hat{U}_{JK}}{\hat{c}_{JK}} \vec{u}_{JK} \Delta_{JK} U = 0. \quad (\text{B.3c})$$

The contributions to the numerical dissipation term associated to the contact wave appear in (B.3b), while contributions associated to the acoustic waves are those in (B.3c).

Total energy equations

$$\delta \frac{d(\alpha_k E_k)_J}{dt} + \frac{1}{2} \sum_{K \in \nu(J)} ((\alpha_k E_k)_K + (\alpha_k p_k)_K) \vec{u}_K \cdot \vec{n}_{JK} \quad (\text{B.4a})$$

$$+ \frac{1}{2} \sum_{K \in \nu(J)} |\hat{U}_{JK}| \left( -\widehat{Y}_k \widehat{H}_{kJK} \frac{\Delta_{JK} p_m}{\hat{c}_{JK}^2} + \Delta_{JK} (\alpha_k \mathcal{E}_k) + M_*^2 \left( \frac{\hat{U}_{JK}^2 + \hat{V}_{JK}^2}{2} \Delta_{JK} (\alpha_k \rho_k) + \hat{\rho}_{JK} \widehat{V} \widehat{Y}_{kJK} \Delta_{JK} V \right) \right) \quad (\text{B.4b})$$

$$+ \frac{1}{2M_*} \sum_{K \in \nu(J)} \widehat{Y}_k \widehat{H}_{kJK} \frac{\Delta_{JK} p_m}{\hat{c}_{JK}} + \frac{M_*}{2} \sum_{K \in \nu(J)} \widehat{U} \widehat{Y}_{kJK} \frac{\hat{U}}{\hat{c}} \Delta_{JK} p_m + \left( \widehat{Y}_k \widehat{H}_{kJK} \frac{\hat{U}_{JK}}{\hat{c}_{JK}} + \widehat{U} \widehat{Y}_{kJK} \hat{c}_{JK} \right) \hat{\rho}_{JK} \Delta_{JK} U \quad (\text{B.4c})$$

$$+ \frac{(-1)^k}{2} \sum_{K \in \nu(J)} (\widehat{U} \widehat{Y}_{2JK} \gamma_1 \varpi_1 + \widehat{U} \widehat{Y}_{1JK} \gamma_2 \varpi_2) \Delta_{JK} \alpha_1 + M_*^2 \left( C_{JK} + \kappa_1 \widehat{U} \widehat{Y}_{2JK} \frac{\hat{U}_{JK}^2 + \hat{V}_{JK}^2}{2} \right) \Delta_{JK} (\alpha_1 \rho_1) \quad (\text{B.4d})$$

$$+ M_*^2 \left( C_{JK} - \kappa_2 \widehat{U} \widehat{Y}_{1JK} \frac{\hat{U}_{JK}^2 + \hat{V}_{JK}^2}{2} \right) \Delta_{JK} (\alpha_2 \rho_2) - \chi_1 \widehat{U} \widehat{Y}_{2JK} \Delta_{JK} (\alpha_1 \rho_1) + \chi_2 \widehat{U} \widehat{Y}_{1JK} \Delta_{JK} (\alpha_2 \rho_2) \quad (\text{B.4e})$$

$$+ M_*^2 \widehat{U} \widehat{Y}_{1JK} \widehat{U} \widehat{Y}_{2JK} (\kappa_1 - \kappa_2) \Delta_{JK} (\rho U) - \kappa_1 \widehat{U} \widehat{Y}_{2JK} \Delta_{JK} (\alpha_1 E_1) + \kappa_2 \widehat{U} \widehat{Y}_{1JK} \Delta_{JK} (\alpha_2 E_2) \quad (\text{B.4f})$$

$$+ M_*^2 (\kappa_1 \widehat{U} \widehat{Y}_{2JK} \widehat{V} \widehat{Y}_{1JK} - \kappa_2 \widehat{U} \widehat{Y}_{1JK} \widehat{V} \widehat{Y}_{2JK}) \Delta_{JK} (\rho V) = 0, \quad k = 1, 2, \quad (\text{B.4g})$$

$$\text{where } C_{JK} = -\kappa_1 \widehat{U} \widehat{Y}_{2JK} (\hat{U}_{JK} \widehat{U} \widehat{Y}_{1JK} + \hat{V}_{JK} \widehat{V} \widehat{Y}_{1JK}) + \kappa_2 \widehat{U} \widehat{Y}_{1JK} (\hat{U}_{JK} \widehat{U} \widehat{Y}_{2JK} + \hat{V}_{JK} \widehat{V} \widehat{Y}_{2JK}). \quad (\text{B.4h})$$

The contributions to the numerical dissipation term associated to the contact wave appear in (B.4b), while contributions associated to the acoustic waves are those in (B.4c). The terms in (B.4d)-(B.4g) correspond to the Roe linearization of the non-conservative products in the phasic total energy equations.

### Appendix C. Transformation matrix for the six-equation two-phase model

We consider for simplicity the one-dimensional case with  $q = [\alpha_1, \alpha_1 \rho_1, \alpha_2 \rho_2, \rho u, \alpha_1 E_1, \alpha_2 E_2]^T$ , and  $\varphi = [p_m, u, s_1, s_2, Y_1, \alpha_1]^T$ . We consider species governed by the stiffened gas EOS, with the pressure law in Section 2 and the caloric law  $T_k(p_k, \rho_k) = (p_k + \varpi_k)/(C_{vk} \rho_k (\gamma_k - 1))$ ,  $C_{vk} = \text{const}$ . The transformation matrix is found as:

$$\frac{\partial \varphi}{\partial q} = \begin{pmatrix} -\gamma_1 \varpi_1 + \gamma_2 \varpi_2 & \chi_1 - \kappa_1 (1 - 2Y_1) \frac{u^2}{2} & \chi_2 + \kappa_1 Y_1 u^2 & -(\kappa_1 Y_1 + \kappa_2 Y_2) u & \kappa_1 & \kappa_2 \\ & +\kappa_2 Y_2 u^2 & -\kappa_2 (1 - 2Y_2) \frac{u^2}{2} & & & \\ 0 & -\frac{u}{\rho} & -\frac{u}{\rho} & \frac{1}{\rho} & 0 & 0 \\ \frac{p_1}{T_1 \rho Y_1} & -\frac{H_1}{T_1 \rho Y_1} + \frac{u^2}{T_1 \rho} & \frac{u^2}{T_1 \rho} & -\frac{u}{T_1 \rho} & \frac{1}{T_1 \rho Y_1} & 0 \\ -\frac{p_2}{T_2 \rho Y_2} & \frac{u^2}{T_2 \rho} & -\frac{H_2}{T_2 \rho Y_2} + \frac{u^2}{T_2 \rho} & -\frac{u}{T_2 \rho} & 0 & \frac{1}{T_2 \rho Y_2} \\ 0 & \frac{Y_2}{\rho} & -\frac{Y_1}{\rho} & 0 & 0 & 0 \\ 1 & 0 & 0 & 0 & 0 & 0 \end{pmatrix}.$$

## References

- [1] M. Pelanti, K.-M. Shyue, A mixture-energy-consistent six-equation two-phase numerical model for fluids with interfaces, cavitation and evaporation waves, *J. Comput. Phys.* 259 (2014) 331–357.
- [2] R. Saurel, F. Petitpas, R. A. Berry, Simple and efficient relaxation methods for interfaces separating compressible fluids, cavitating flows and shocks in multiphase mixtures, *J. Comput. Phys.* 228 (2009) 1678–1712.
- [3] M. Pelanti, K.-M. Shyue, A mixture-energy-consistent numerical approximation of a two-phase flow model for fluids with interfaces and cavitation, in: F. Ancona, A. Bressan, P. Marcati, A. Marson (Eds.), *Hyperbolic Problems: Theory, Numerics, Applications, Proc. 14th Intl. Conf. on Hyperbolic Problems, AIMS, 2014*, pp. 839–846.
- [4] M. R. Baer, J. W. Nunziato, A two-phase mixture theory for the deflagration-to-detonation transition (DDT) in reactive granular materials, *Intl. J. Multiphase Flows* 12 (1986) 861–889.
- [5] A. Kapila, R. Menikoff, J. B. Dzil, S. F. Son, D. Stewart, Two-phase modeling of deflagration-to-detonation transition in granular materials: Reduced equations, *Physics of Fluids* 13 (2001) 3002–3024.
- [6] R. Saurel, R. Abgrall, A multiphase Godunov method for compressible multifluid and multiphase flows, *J. Comput. Phys.* 150 (1999) 425–467.
- [7] S. Klainerman, A. Majda, Compressible and incompressible fluids, *Commun. Pure Appl. Math* 35 (1982) 629–651.
- [8] G. Volpe, Performance of compressible flow codes at low Mach number, *AIAA J.* 31 (1993) 49–56.
- [9] E. Turkel, Preconditioned methods for solving the incompressible and low speed compressible equations, *J. Comput. Phys.* 72 (1987) 277–298.
- [10] B. van Leer, W. Lee, P. Roe, Characteristic time-stepping or local preconditioning of the Euler equations, 1991. *AIAA Paper 1991-1552*.
- [11] J. Sesterhenn, B. Müller, H. Thomann, On the cancellation problem in calculating compressible low Mach number flows, *J. Comput. Phys.* 151 (1999) 597–615.
- [12] H. Guillard, C. Viozat, On the behaviour of upwind schemes in the low Mach number limit, *Computers and Fluids* 28 (1999) 63–86.
- [13] H. Guillard, A. Murrone, On the behaviour of upwind schemes in the low Mach number limit: II. Godunov-type schemes, *Computers and Fluids* 338 (2004) 655–675.
- [14] H. Paillère, C. Viozat, A. Kumbaro, I. Toumi, Comparison of low Mach number models for natural convection problems, *Heat and Mass Transfer* 36 (2000) 567–573.
- [15] X.-S. Li, C.-W. Gu, An all-speed Roe-type scheme and its asymptotic analysis of low Mach number behaviour, *J. Comput. Phys.* 227 (2008) 5144–5159.
- [16] X.-S. Li, C.-W. Gu, J.-Z. Xu, Development of Roe-type scheme for all-speed flows based on preconditioning method, *Computers and Fluids* 38 (2009) 810–817.
- [17] B. J. R. Thornber, D. Drikakis, Numerical dissipation of upwind schemes in low Mach flow, *Int. J. Numer. Meth. Fluids* 56 (2008) 1535–1541.
- [18] S. Dellacherie, Analysis of Godunov type schemes applied to the compressible Euler system at low Mach number, *J. Comput. Phys.* 229 (2010) 978–1016.
- [19] P. Degond, M. Tang, All speed scheme for the low Mach number limit of the isentropic Euler equations, *Communications in Computational Physics* 10 (2011) 1–31.
- [20] F. Rieper, A low-Mach number fix for Roe’s approximate Riemann solver, *J. Comput. Phys.* 230 (2011) 5263–5287.
- [21] X.-S. Li, C.-W. Gu, Mechanism of Roe-type schemes for all-speed flows and its application, *Computers and Fluids* 86 (2013) 56–70.
- [22] R. Klein, N. Botta, T. Schneider, C. D. Munz, S. Roller, A. Meister, L. Hoffmann, T. Sonar, Asymptotic adaptive methods for multi-scale problems in fluid mechanics, *J. Engrg. Math.* 39 (2001) 261–343.
- [23] J. Haack, S. Jin, J.-G. Liu, An all-speed Asymptotic-Preserving method for the isentropic Euler and Navier–Stokes equations, *Commun. Comput. Phys.* 12 (2012) 955–980.
- [24] R. Klein, Semi-implicit extension of a Godunov-type scheme based on low Mach number asymptotics. I. One-dimensional flow, *J. Comput. Phys.* 121 (1995) 213–237.
- [25] S. Noelle, G. Bispen, K. R. Arun, M. Lukáčová-Medvid’ová, C.-D. Munz, An asymptotic preserving all Mach number scheme for the Euler equations of gas dynamics, *SIAM J. Sci. Comp.* 36 (2014) B989–B1024.
- [26] F. Moukalled, M. Darwish, B. Seka, A pressure-based algorithm for multi-phase flow at all speeds, *J. Comput. Phys.* 190 (2003) 550–571.
- [27] S. Venkateswaran, J. Lindau, R. F. Kunz, C. Merkle, Computation of multiphase mixture flows with compressibility effects, *J. Comput. Phys.* 180 (2000) 54–77.
- [28] A. Murrone, H. Guillard, Behavior of upwind scheme in the low Mach number limit: III. Preconditioned dissipation for a five equation two phase model, *Computers and Fluids* 37 (2008) 1209–1224.
- [29] B. Braconnier, B. Nkonga, An all-speed relaxation scheme for interface flows with surface tension, *J. Comput. Phys.* 228 (2009) 5722–5739.
- [30] S. LeMartelot, B. Nkonga, R. Saurel, Liquid and liquid-gas flows at all speeds, *J. Comput. Phys.* 255 (2013) 53–82.

- [31] H. Guillard, On the behavior of upwind schemes in the low Mach number limit. IV: P0 approximation on triangular and tetrahedral cells, *Computers and Fluids* 38 (2009) 1969–1972.
- [32] E. Turkel, Review of preconditioning methods for fluid dynamics, *Appl. Numer. Math.* 12 (1993) 257–284.
- [33] Y.-H. Choi, C. Merkle, The application of preconditioning in viscous flows, *J. Comput. Phys.* 105 (1993) 207–223.
- [34] D. L. Darmofal, B. van Leer, Local preconditioning: Manipulating mother nature to fool father time, in: D. A. Caughey, M. M. Hafez (Eds.), *Frontiers of Computational Fluid Dynamics*, World Scientific Publishing, 1998, pp. 211–239.
- [35] C. Viozat, Implicit upwind schemes for low Mach number compressible flows, INRIA Report 3084, 1997.
- [36] P. Birken, A. Meister, On low Mach number preconditioning of finite volume schemes, *Proc. Appl. Math. Mech.* 5 (2005) 759–760.
- [37] G. H. Schnerr, I. H. Sezal, S. J. Schmidt, Numerical investigation of three-dimensional cloud cavitation with special emphasis on collapse induced shock dynamics, *Phys. Fluids* 20 (2008). 040703.
- [38] M. Bilanceri, F. Beux, M. V. Salvetti, An implicit low-diffusive HLL scheme with complete time linearization: Application to cavitating barotropic flows, *Computers and Fluids* 39 (2010) 1990–2006.
- [39] E. Goncalves, R. F. Patella, Numerical simulation of cavitating flows with homogeneous models, *Computers and Fluids* 38 (2009) 1682–1696.
- [40] S. Clerc, Numerical simulation of the homogeneous equilibrium model for two-phase flow, *J. Comput. Phys.* 161 (2000) 354–375.
- [41] A. Zein, M. Hantke, G. Warnecke, Modeling phase transition for compressible two-phase flows applied to metastable liquids, *J. Comput. Phys.* 229 (2010) 2964–2998.
- [42] A. B. Wood, A textbook of sound, G. Bell and Sons Ltd., London, 1930.
- [43] R. J. LeVeque, Wave propagation algorithms for multi-dimensional hyperbolic systems, *J. Comput. Phys.* 131 (1997) 327–353.
- [44] R. J. LeVeque, *Finite Volume Methods for Hyperbolic Problems*, Cambridge University Press, 2002.
- [45] R. J. LeVeque, *CLAWPACK V.4.3*, 2006. <http://www.clawpack.org>.
- [46] E. F. Toro, *Riemann Solvers and Numerical Methods for Fluid Dynamics*, Springer-Verlag, 1997.
- [47] P. L. Roe, Approximate Riemann solvers, parameter vectors, and difference schemes, *J. Comput. Phys.* 43 (1981) 357–372.
- [48] E. F. Toro, M. Spruce, W. Speares, Restoration of the contact surface in the HLL Riemann solver, *Shock Waves* 4 (1994) 25–34.
- [49] S. F. Davis, Simplified second-order Godunov-type methods, *SIAM J. Sci. Stat. Comput.* 9 (1988) 445–473.
- [50] R. Klein, Semi-implicit extension of a Godunov-type scheme based on low Mach number asymptotics. I: one-dimensional flow, *J. Comput. Phys.* 121 (1995) 213–237.
- [51] B. Müller, Low-Mach-number asymptotics of the Navier-Stokes equations, *J. Engrg. Math.* 34 (1998) 97–109.
- [52] B. Müller, Low Mach number asymptotics of the Navier-Stokes equations and numerical implications, 1999. 30th Computational Fluid Dynamics Lecture Series, von Karman Institute for Fluid Dynamics.
- [53] J. H. Park, C.-D. Munz, Multiple pressure variables methods for fluid flow at all Mach numbers, *Int. J. Numer. Meth. Fluids* 49 (2005) 905–931.
- [54] R. A. Berry, R. Saurel, O. Le Métayer, The discrete equation method (DEM) for fully compressible, two-phase flows in ducts of spatially varying cross-section, *Nuc. Eng. Des.* 240 (2010) 3797–3818.
- [55] B. Charrière, J. Decaix, E. Goncalvès, A comparative study of cavitation models in a Venturi flow, *Eur. J. Mech. B Fluid* 49 (2015) 287–297.
- [56] O. Coutier-Delgosha, B. Stutz, A. Vabre, S. Legoupil, Analysis of cavitating flow structure by experimental and numerical investigations, *J. Fluid Mech.* 578 (2007) 171–222.
- [57] S. LeMartelot, R. Saurel, O. Le Métayer, Steady one-dimensional nozzle flow solutions of liquid-gas mixtures, *J. Fluid Mech.* 737 (2013) 146–175.
- [58] T. Kloczko, C. Corre, A. Beccantini, Low-cost implicit schemes for all-speed flows on unstructured meshes, *Int. J. Numer. Meth. Fluids* 58 (2008) 493–526.